UNIVERSITY OF CALIFORNIA, SAN DIEGO

Screening and Characterization of Polyhydroxyalkanoate and other Granules in Cyanobacteria

A thesis submitted in partial satisfaction of the
requirements for the degree Master of Science

in

Biology

by

Karl Bryant Hong

Committee in charge:

Professor Brian Palenik, Chair
Professor James Golden, Co-Chair
Professor Stephen Mayfield

2017

The thesis of Karl Bryant Hong is approved and it is accepted in quality and form for publication on microfilm and electronically

_____

_____

Co-Chair

_____

Chair

University of California, San Diego

2017

DEDICATION

I dedicate this work to my mom and dad, who by example taught me the power of love, and the audacity to dream.

TABLE OF CONTENTS

Signature Page……. iii

Dedication……. iv

Table of Contents……. v

List of Figures……. vii

List of Tables……. x

Acknowledgements……. xi

Abstract of the Thesis……. xii

Introduction……. 1
1. Environmental Challenges Posed by Plastics and other Petroleum Products……. 1
2. Biotechnology from Cyanobacteria……. 2
3. Cyanobacterial Storage Products (PHA, LD, NRP) ……. 3
3.1 Polyhydroxyalkanoates……. 3
3.2 Neutral Lipid Droplets……. 7
3.3 Non-ribosomal Peptides and Polyamides……. 9

Materials and Methods……. 13
1. Phylogenetic Methods……. 13
2. Culture conditions……. 16
3. Staining and Counting of Granules……. 17
4. Proton NMR……. 18
5. FTIR……. 19
6. Lipid Analysis……. 19
7. Purification of CGP-like granules in Nodularia sp. Las Olas……. 21
8. HPLC Amino Acid Analysis……. 21

TABLE OF CONTENTS

Results…… 23
1. Screening of Cyanobacteria for PHA and other Hydrophobic Granules 23
2. ^{1}H NMR Spectroscopy of Staining Strains…… 24
3. Phylogenetic Analysis of Polyhydroxyalkanoate Synthase Gene phaC… 27
3.1Contextualizing Screening Results with 16s and 23s rRNA Phlogeny…… 27
3.2 Genetic Survey of PHA Biosynthesis Operons …… 28
3.3 Cophylogenetic Analysis of phaE/phaC and 16s/23s rRNA Phylogenies…… 30
4. Accumulation and Degradation of Granules in Nodularia sp. Las Olas… 34
4.1 Effects of Salinity on Accumulation and Degradation of Granules…… 34
4.2 Effects of Nitrogen and Phosphate Limitation on Accumulation of Granules…… 39
4.3 Effect of Light Limitation on Accumulation of Granules…… 39
5. FTIR Analysis of Nodularia sp. Las Olas cell pellets…… 43
6. LC-MS Amino Acid Analysis of Nodularia sp. Las Olas Cell Pellets…… 44
7. GC-MS and TLC analyses of Nodularia sp. Las Olas and Phormidium cf. irriguum CCALA 759 Lipid Extracts…… 49

Discussion…… 59
1. Characterization of Polyhydroxyalkanoates…… 59
2. Characterization of Granules in Nodularia sp. Las Olas…… 61
3. Characterization of Granules in Phormidium cf. irriguum CCALA 759.. 66

References…… 69

LIST OF FIGURES

Figure 1: Bodipy 493/503 staining of representative cyanobacteria strains. Staining granules appear green, whereas chlorophyll autofluorescence appears red…….,,,,,……..... 23

Figure 2: ^{1}H NMR of hydrophobic extracts from representative cyanobacteria strains. The non-staining, phaC negative strain Nodularia sp. WHNOD was analyzed as a negative control. Purified PHB was analyzed as a standard. The X-axis shows chemical shifts in parts per million (ppm). …… 26

Figure 3: a maximum likelihood phylogeny of cyanobacterial 16s and 23s rRNA genes. Bootstrap values are indicated at each node……..... 28

Figure 4a: TreeMap co-phylogeny of maximum likelihood 16s/23s rRNA and phaC/phaE gene trees. Bootstrap values are indicated at each node. PHB producers characterized in this study are in bold, and strains with incongruent phylogenies are indicated by red text. ……..... 31

Figure 4b: Maximum likelihood 16s and 23s rRNA gene of cyanobacteria with phaC genes. This tree was used to construct Figure 4a. …….. 32

Figure 4c: Maximum likelihood cyanobacterial phaC and phaE gene tree used to construct Figure 4a. ……..... 32

Figure 5: The four best co-phylogenetic reconstructions of the given cyanobacteria 16s/23s and phaE/phaC trees according to JANE (top). A legend, as well as a distribution of costs for a random sample of solutions is also shown (bottom)…….. 34

Figure 6a: Granules per cell of Nodularia sp. Las Olas grown in F/2 media with variable salinity. Data shown are averages from four replicates. Error bars show 95 percent confidence intervals. Chla fluorescence of said cultures are included as a measurement of growth. ……..... 36

Figure 6b: Granules per cell of Nodularia sp. Las Olas grown in F/2 media with variable salinity, including an additional pair of cultures grown at 150% salinity using Red Sea salts. Both replicates are shown. All other data are averages from four replicates. Error bars show 95 percent confidence intervals. …… 37

Figure 7: Degradation of staining granules under salt shock conditions by Nodularia sp. Las Olas. Two replicates for each treatment are shown. …… 38

LIST OF FIGURES

Figure 8: Granules per cell and Chla fluorescence of Nodularia sp. Las Olas over time. Two replicates for each treatment are shown. 40

Figure 9: The number of granules per cell of Nodularia sp. Las Olas cultures grown in F/2 media made from 100% seawater, under different nitrogen conditions. Two replicates for each treatment are shown. 41

Figure 10: Granules per cell of salt-shocked Nodularia sp. Las Olas accompanied by Chla fluorescence of salt-shocked cultures. Data shown are averages from four replicates. Error bars show 95% confidence intervals. 42

Figure 11: FTIR spectra of staining and non-staining cultures of Nodularia sp. Las Olas. 43

Figure 12: Percent amino acid composition by mole of whole Nodularia sp. Las Olas cell pellets grown in 10%, 50%, and 150% seawater. Due to acid hydrolysis, aspartate and asparagine content is listed as "Asx", and glutamate and glutamine content is listed as "Glx". 44

Figure 13: Amino acid composition of water-insoluble cell fraction following French pressure cell treatment and two water washes. 46

Figure 14: Amino acid composition of final cell pellets insoluble in water, 2% triton-X 100, and 0.1N HCl. 47

Figure 15: Amino acid composition of 0.1 N HCl extracts containing CGP-like granules. 48

Figure 16: BODIPY 493/503 staining of cell pellets subject to amino acid analysis..... 49

Figure 17: GC-MS spectra of lipid extracts from Nodularia sp. WHNOD and Nodularia sp. Las Olas grown at 10% and 150% salinity. Integrated areas of significant peaks are color-coded, beside each peak. Peak labels are based on NIST library searches, and are consistent across all samples..... 52

Figure 18: GC-MS spectra of a second, more dilute pair of lipid extracts from Nodularia sp. Las Olas cultures grown at 10% and 150% salinity, extracted with 500ul instead of 330 µl hexanes. Integrated areas of significant peaks are color-coded beside each peak. Peak labels are based on NIST library searches... 53

LIST OF FIGURES

Figure 19: GC-MS spectra of lipid extracts from Phormidium cf. irriguum CCALA 759 and Phormidium autumnale UTEX 1580. Integrated areas of significant peaks are color-coded beside each peak. Peak labels are based on NIST library searches, and are consistent across all samples…… 54

Figure 20: TLC plates of Nodularia sp. Las Olas at 10% and 150% salinity, UTEX 1580, CCALA 759, Nodularia sp. WHNOD, and vegetable oil using a two-solvent system…….. 55

Figure 21: GC-MS spectra of TLC spot 1 (as labeled in Figure 19)…….. 56

Figure 22: GC-MS spectra of TLC spot 2 (as labeled in Figure 19)…… 57

Figure 23: GC-MS spectra of TLC spot 3 (as labeled in Figure 19) …….. 57

Figure 24: GC-MS spectra of TLC spot 3 (as labeled in Figure 19) …….. 58

LIST OF TABLES

Table 1: Strains and DNA sequences in this study…….…….…….…….. 13

Table 2: Jane (version 4) default cost values used in this study…….…….. 16

Table 3: Summary of PhaC Screening Results 23…….…….…….…….. 24

Table 4: PHA Biosynthesis operon topology 29…….…….…….…….. 29

Acknowledgements

I would like to acknowledge Professor Brian Palenik for his support and guidance throughout this project, as chair of my committee.

I would also like to acknowledge members of Professor Michael D. Burkart's lab, Joris Beld and Tony Davis for their assistance and training with ^{1}H NMR spectroscopy, as well as Jeffrey Minrebo for his assistance and training with gas chromatography-mass spectrometry.

I would also like to acknowledge Christopher Dupont for his assistance and training with FTIR spectroscopy.

The LC-MS amino acid analysis presented in Figure 12 was optimized and prepared with help from Rasmus Swalethorpe from Dr. Lihini Aluwihare's lab.

Results are currently being prepared for submission for publication of the material. Hong, Karl; Palenik, Brian. The thesis author was the primary author of this material, under the guidance of the principal investigator, Brian Palenik.

Abstract of the Thesis

Screening and Characterization of Polyhydroxyalkanoate and other Granules in Cyanobacteria

by

Karl Bryant Hong

Master of Science in Biology

University of California, San Diego, 2017

Professor Brian Palenik, Chair
Professor James Golden, Co-Chair

Using Nile Red and Bodipy 493/503 dyes and fluorescence microscopy, twenty cyanobacterial strains were screened for the accumulation of potentially biotechnologically significant granules such as polyhydroxybutyrate (PHB). Six of

these strains showed such granules, including the five recent isolates, *Synechocystis* spp. *WHSYN*, *LSNM*, and *CGF*-1, *Nodularia* sp. *Las Olas,* and *Phormidium*-like sp. *CGFILA*, as well as *Phormidium* cf. *irriguum* CCALA 759. Characterizations of these granules reveal that they belong to three distinct classes of cyanobacterial carbon storage compounds. *Synechocystis,* spp. *WHSYN, LSNM,* and *CGF-1*, and *Phormidium*-like sp. *CGFILA* produce polyhydroxyalkanoate (PHA) granules according to PHA synthase gene (*phaC*) PCR screening and ^{1}H NMR analyses. Maximum-likelihood analyses and co-phylogenetic modeling of PHA synthase gene sequences provide evidence of a recent horizontal gene transfer event between distant genera of cyanobacteria. The data set includes the first genetic characterization of a PHA biosynthesis gene from the genus *Phormidium,* and it also reveals that *phaC* is highly conserved within the genus *Synechocystis*.

Another strain, *Phormidium* cf. *irriguum* CCALA 759 was found to not produce PHA, but produce staining granules possibly comprised of hexadecanoic and octadecanoic fatty acids (84.7% and 75.8% probability NIST matches, respectively), as well as alkanes which have tentatively been identified as 8-heptadecene via gas chromatography-mass spectrometry (two peaks, 15.8% and 18.6% probability NIST matches).

A third granule type was found in *Nodularia* sp. *Las Olas* and appears to be poly-amino acids comprised mainly of arginine and aspartate/asparagine residues, according to Fourier-transform infrared spectroscopy and high performance liquid

chromatography analyses. This poly-amino acid material exhibits staining and solubility characteristics that are different from cyanophycin controls.

Introduction

1. Environmental Challenges Posed by Plastics and other Petroleum Products

Petroleum products are a cornerstone of modern life, their uses ranging from energy and fuel, to plastics, pharmaceuticals, and other modern materials. However, these products are not renewable, and their use and disposal often causes environmental harm. In order to continue to enjoy the lifestyles afforded to us by these products, there is a need to develop green, renewable, and biodegradable alternatives to petroleum products

The combustion of fossil fuels for energy and transportation is the single largest contributor for carbon dioxide emissions in the United States, accounting for roughly 77 percent of greenhouse gas emissions since 1990, when weighted according to their global warming potential (1). In 2015, nearly half of the carbon dioxide emitted via combustion was due to the use of transportation fuels (1), which prove especially difficult to replace due to their requirement for high energy density, and the need to be compatible with existing infrastructure.

The accumulations of waste plastics are another major health and environmental concern. In 2010, an estimated 257 million metric tons of waste plastics were generated worldwide, much of which was improperly disposed of (2). Due to their lack of biodegradability, these waste plastics are extremely long-lived and persistent in the environment. Large plastic debris can physically harm marine life via entanglement or ingestion; however even small microplastics have the

potential to introduce toxic substances into the food chain when ingested, posing a risk both to animal and human health (3, 4). These microplastics are produced via photochemical degradation of larger plastics, which is the primary mechanism of waste plastic degradation in the environment (3, 5). Thus, there is a need to develop alternative biodegradable plastics in order to reduce the health and environmental impact of our waste streams.

2. Biotechnology from Cyanobacteria

The phylum Cyanobacteria consists of gram-negative photosynthetic bacteria, which possess great potential for biotechnological use in meeting these challenges. Cyanobacteria share many advantages of bacterial systems, such as ease of genetic manipulation, short life cycles, and the natural transformability (6), in addition to high genetic and metabolic diversity (7–9).

Many cyanobacteria can also fix nitrogen both for themselves and as bio-fertilizers, which reduces nutrient requirements (10). Unlike other bacteria, however, cyanobacteria can obtain the carbon necessary for effective cultivation and carbon storage compound production via photosynthesis, without fertilization with refined carbon sources (11, 12).

Furthermore, cyanobacteria can be grown in a wide range of pH, salinity, and temperature environments which allow cultivation in marginal land and water where other agricultural organisms cannot be grown (6).

Finally, cyanobacteria are naturally capable of producing a number of useful lipids, polymers, and secondary metabolites, which can be used to replace certain petroleum products with renewable alternatives that have reduced carbon footprints. Such compounds are often accumulated as granular inclusions in cyanobacteria, which can be harvested and converted into a variety of commercial products such as biofuels and bioplastics.

Three major classes of these inclusions are polyhydroxyalkanoates (PHAs), neutral lipid droplets (LDs), and non-ribosomal polypeptides (NRPs). Two of these inclusions, PHAs and LDs, are typically detected using the fluorescent stains Nile Red and BODIPY 493/503 (13, 14). Although non-ribosomal polypeptides (NRPs) are not typically associated with these neutral lipid dyes, this study characterizes a BODIPY 493/503-staining granule, which appears to contain a cyanophycin-like poly-arginine and poly-aspartate/asparagine component.

This study aims to chemically and phylogenetically characterize the Nile Red and BODIPY 493/503-staining granules found via screening of twenty cyanobacteria from the genera *Phormidium*, *Oscillatoria*, *Synechocystis*, and *Nodularia*. Table 1 lists strains and DNA sequences used in this study.

3. Cyanobacterial Storage Products (PHA, LD, NRP)

3.1 Polyhydroxyalkanoates

Polyhydroxyalkanoates are a class of carbon storage compounds found in bacteria. Research on PHAs has been focused mainly on their potential to be

converted into biodegradable and renewable plastics. Cyanobacteria are a logical choice for the production of PHAs because some can natively synthesize PHAs from atmospheric carbon fixed via oxygenic photosynthesis, without the need to be fertilized with organic carbon sources (11). In addition to the other advantages of cyanobacterial cultivation mentioned previously, photosynthetic PHA biosynthesis would also allow for carbon dioxide cycling, potentially lowering the carbon footprints associated with PHA production.

PHAs are semi-crystalline polymers which can be described by the formula, $(O\text{-}CHR\text{-}CH_2\text{-}C{=}O)_n$, where R represents an alkyl side chain (15). PHAs are generally classified as either short chain length polymers (SCL-PHA) consisting of 3-5 carbon monomers, or medium chain length polymers (MCL-PHA) consisting of 6-15 carbon monomers, with different enzymes generally responsible for the synthesis degradation of each (16, 17).

The SCL-PHA, poly-3-hydroxybutyrate (PHB) is the most common PHA found in nature; however, different short and medium chain length PHAs and PHA co-polymers with varying chemical and physical properties have also been found in bacteria (15, 18). In general, short chain length PHAs tend to form stiff and brittle crystalline structures, whereas medium chain length PHAs tend to be more elastiomeric (19). In a rare case, *Pseudomonas* sp. possesses PHA synthase genes capable of producing co-polymers of short and medium chain length PHAs (20). These SCL-MCL PHA copolymers possess a combination of these aforementioned traits, increasing the potential utility of PHA bioplastics (21). SCL-MCL PHA co-

polymers are not the only PHA co-polymers observed in nature, however. Co-polymers of different SCL-PHAs have also been found in nature, possessing characteristics that are different from than PHA homopolymers. Notably, many cyanobacteria also produce co-polymers of PHB and Poly-B-hydroxyvalerate (PHV) especially when grown in the presence of propionate (22, 23). These SCL-PHA co-polymers were found to possess better thermal stability and elasticity but lower tensile strength than PHB homopolymers (24).

Cyanobacteria accumulate PHAs as granules consisting of a hydrophobic PHA core that is surrounded by associated proteins (25). These granules are typically accumulated under nutrient-limited conditions. In particular, nitrogen limitation is a well-studied inducer of PHA accumulation, and phosphate limitation has also been observed to increase PHA accumulation in cyanobacteria (26)(27). Salt stress, photoperiod, temperature, pH, and the presence of organic carbon sources are also affect PHA accumulation, albeit less drastically (27).

Cyanobacterial PHAs are synthesized from acetyl-coA via three chemical reactions, each catalyzed by a different enzyme. In the first reaction, the enzyme B-ketothiolase catalyzes the combination of acetyl-coA molecules to form acetoacetyl-coA. In the second reaction, the enzyme acetoacetyl-CoA reductase reduces the acetoacetyl-CoA molecule to form a hydroxyalkanoate-CoA monomer. Finally, PHA synthase catalyzes the polymerization of these monomers to form a polyhydroxyalkanoate (28).

The three enzymes, B-ketothiolase, Acetoacetyl-CoA reductase, and PHA synthase are encoded by the following four genes: *phaA, phaB, phaC*, and *phaE*. *PhaA* codes for B-ketothiolase and *phaB* codes for Acetoacetyl-coA reductase (28). P*haC* and *phaE* each code for one of the two components of PHA synthase (28). In cyanobacteria, these four genes may be arranged within one or two operons (Table 2).

Cyanobacterial PHA synthase is structurally similar to that of gram-negative purple sulfur bacteria, which also possess two-component PHA synthases (29). Indeed, the PHA biosynthesis genes of several purple sulfur bacteria appear to be the closest non-cyanobacterial relatives to genes described in this study according to sequences found using NCBI BLAST. Previous studies show evidence of deep horizontal gene transfer (HGT) of PHA biosynthesis genes between cyanobacteria and other bacterial clades (30); however, little has been done to investigate HGT and phylogenetic relationships of *phaC* genes within the phylum Cyanobacteria.

Perhaps the most significant advantage of PHB bioplastics over traditional plastics is their biodegradability. The durability and persistence of traditional plastics and plastic products poses significant environmental and health risks (3, 31). While it is generally estimated that traditional plastics take hundreds of years to degrade, disposable bottles made from PHA bioplastics are estimated to fully degrade on the order of 5-10 years in situ (32). This is likely due to the widespread occurrence of organisms able to break down PHAs as an energy source.

Because the occurrence of PHA biosynthesis is so common among bacteria, it is only natural that the enzymes responsible for breaking them down are also extremely common. PHA depolymerases are grouped into four main families specialized for either extracellular or intracellular degradation of short or medium chain length PHAs (17). While intracellular PHA depolymerases are specialized for the catabolism of intracellular PHA granules, extracellular PHA depolymerases are typically secreted into the environment to facilitate the breakdown of PHAs found in the cell's environment (33). Such extracellular PHA depolymerases are quite common among fungi (34, 35) and bacteria (33), including many cyanobacteria (17).

PHA biomaterials have other useful properties. Compared to starch-based bioplastics, PHA bioplastics tend to have superior hydrophobicity (19). Other favorable properties include thermoplasticity, low vapor-permeability, and biocompatibility, making PHA bioplastics especially suitable for biomedical and food packaging purposes (36–39). PHA polymers can be used medically as implants and drug delivery carriers, or they can be broken down into monomers which can either be converted into pharmaceuticals, or directly administered to patients (40). As a medicine, the direct administration of PHA monomer ketone bodies has been shown to have neuroprotective effects in mice and rats with degenerative brain conditions (41–44).

3.2 Neutral Lipid Droplets

Lipids from photosynthetic organisms can be converted into liquid fuels such as gasoline, diesel, and jet fuel that are environmentally responsible, renewable, and compatible with existing vehicles (45–48). These lipids, often triacylglerols, are typically stored as Neutral lipid droplets (LDs) within the cell. LDs are a class of carbon storage compounds present across all domains of life but less commonly found in bacteria, which tend to accumulate PHAs instead (49). The cultivation of aquatic biomass such cyanobacteria and algae has several advantages over land-based oil crops, such as the ability to be grown on marginal lands and water, as well as the ability to produce much higher yields of oil per acre when compared to terrestrial oil crops such as palm, soy, and jatropha (50).

Typically eukaryotic microalgae are the aquatic biomass of choice for the production of lipids for biofuel use, as they can natively accumulate 50-60% of their dry biomass as lipid (51). However, the relative ease of genetically manipulating of cyanobacteria can help bridge this gap, as well as offer additional prospects such as fatty acid secretion, (52) and nitrogen fixation.

Bacterial lipid droplets tend to be high in triacylglycerides and/or wax esters, consisting of a hydrophobic lipid core surrounded by a phospholipid monolayer (49). The enzymes acyl-ACP reductase (AAR) and aldehyde decarbonylase (ADC), also known as aldehyde deformylating oxygenase (ADO), were shown to be both necessary and sufficient for converting the fatty acyl groups of fatty acyl-acyl carrier proteins into neutral lipid groups in both cyanobacteria and transgenic *E. coli* (53).

Successful efforts to enhance cyanobacterial neutral lipid production tend to focus on the increased expression of these *aar* and *adc* genes (54, 55).

Attempts to enhance the accumulation of cyanobacterial lipids have yielded promising, albeit variable results. Although genetically altered *Synechocystis* sp. PCC 6803 mutants only accumulated up to 1.3% of dry biomass as lipid (55), the LD-producing strain *Nostoc Punctiforme* has more promisingly been genetically altered to accumulate lipids up to 55% dry biomass (54). Thus, neutral lipid production in cyanobacteria can be significant, especially in LD-producing strains that lack PHA biosynthesis genes, such as *N. Punctiforme*. The continued screening of cyanobacteria for LD production expands our genetic toolbox for biofuel production, and increases the likelihood of finding new organisms with high biofuel production potential.

3.3 Non-ribosomal Peptides and Polyamides

Non-ribosomal peptides (NRP) are another class of compounds and polymers found natively in cyanobacteria, consisting of amino acids that have been linked via non-ribosomal biosynthesis. Cyanobacterial NRPs occupy a diverse range of biological roles, ranging from complex toxins (56–59) to relatively simple carbon and nitrogen storage polymers (60, 61). Compared to ribosomal polypeptide synthesis, NRPs can be synthesized without the need for ribosomes and pre-defined templates, allowing amide bonds at carbon chain positions which would not be possible during ribosomal polypeptide synthesis (62). Hybrid NRP

synthases/polyketide synthases have also been characterized in cyanobacteria, enabling the biosynthesis of complex chemicals such as the lipopeptide toxin barbamide, and the cyclic peptide/polyketide hybrids nodularin and microcystin (56, 57, 59). The metabolic diversity afforded by such biosynthetic pathways make cyanobacteria a promising source for the discovery novel natural products, such as pharmaceutical compounds (63).

Cyanophycin granule polypeptides (CGP) are a class of poly-amino acid NRP polymers found in most cyanobacteria, and also in some eubacteria (64, 65). CGPs can typically be described as multi-L-arginyl-poly-(L-aspartic acid) polypeptides consisting of an aspartic acid core upon which arginyl residues are bound in a 1:1 ratio (66). They are commonly observed as cellular inclusions, visible under a light microscope.

The cyanophycin synthetase enzyme is encoded by the gene *CphA*, which has been shown to be sufficient for cyanophycin production in transgenic *E. coli*, albeit with the addition of small amounts of lysine not present in the cyanophycin of *Synechocystis* sp. PCC 6803, from which the gene was cloned (67).

This unexpected incorporation of lysine is consistent with other observations which seem to suggest that cyanophycin synthetase prefers, but is not limited to the use of arginine and aspartic acid as substrates. Specifically, *Synechocystis* sp. 6803 has been shown to incorporate glutamic acid rather than arginine into CGPs under nitrogen-limiting conditions (68), and the phycoerythrin-producing *Synechococcus* sp. strain G2.1 was found to produce cyanophycin granules composed of 29%

arginine, 35% aspartic acid, 15% glutamic acid, and 21% various amino acids (69). Thus, CGP is different from other poly-amino acids found in bacteria such as poly-lysine and poly-glutamic acid, which tend to be comprised of only one peptide (62). This added complexity and chemical diversity further enhances the biotechnological potential of cyanophycin granules.

Cyanophycin accumulation is positively correlated with nitrogenase activity in heterocystic cyanobacteria such as *Cyanothece* sp. strain ATCC51142 (60). In non-heterocystic bacteria such as *Synechocystis* sp. PCC 6803, cyanophycin is also accumulated, but it is affected more by the presence of carbon than it is by nitrogen, possibly due to the use of phycobilisomes as nitrogen storage alternatives (60, 61).

Cyanophycin degradation is mediated by the enzyme cyanophycinase, encoded by the gene *CphB* (70, 71). Like cyanophysin synthetase, cyanophycinase expression is also linked to nitrogen fixation in the heterocystic cyanobacteria *Anabaena* sp. PCC 7120 (70). An extracellular cyanophycinase encoded by the gene *CphE* has also been characterized in the eubacteria *Pseudomonas anguilliseptica* (72), but the occurrence extracellular cyanophycinases is rare according to metagenomic analyses (65).

Cyanophycin and CGP-derived compounds can be used as biopolymers, or as feedstocks for bulk chemical production. CGP polymers are very similar to polyaspartic acids (PASP), and can be further hydrolyzed into homopolymers consisting of only aspartic acid, or co-polymers with higher aspartic acid content (73). Such PASP polymers can serve as biodegradeable alternatives to polyacrylates,

which are widely used as detergents, bioflocculents and anti-scalants (64, 74, 75). The biocompatibility of PASP makes it a good material for the synthesis of biomedical hydro-gels (76, 77). The various amino acids in CGP can also be used as dietary supplements and as renewable feedstocks for the bulk synthesis of nitrogen rich chemicals. (62, 64).

Materials and Methods

1. Phylogenetic Methods

The gene sequences obtained for or used in this study are listed and described in Table 1. Relevant sequences, operon topology, and the relative orientation of the PHB biosynthesis genes were determined using NCBI Genbank's BLAST and "graphics" functions. Sequences without an accession number were obtained via Sanger sequencing using primers described by Hai, et al in 2001 (78), or obtained from the draft genome sequencing of *Synechocystis* sp. *WHSYN*, as part of a different study. Genomes which have been made public in unassembled form were assembled using CLC genomics workbench 8

Table 1: Strains and DNA sequences in this study

NCBI accession number	DNA source	Name of strain
NC_011901.1	NCBI genome	*Thioalkalivibrio sulfidophilus* HL-EbGr7
NC_005125.1	NCBI genome	*Gloeobacter violaceus* PCC 7421
FO818640.1	NCBI genome	*Arthrospira* sp. PCC 8005
NC_016640.1	NCBI genome	*Arthrospira* sp. NIES39
CP013008.1	NCBI genome	*Arthrospira Platensis* YZ
NZ_AFJC01000001.1-01000040.1	NCBI unassembled genome	*Microcoleus vaginatus*
NC_019738.1	NCBI genome	*Microcoleus* sp PCC 7113
NZ_DS989843.1	NCBI genome	*Coleofasciculus chthonoplastes* sp PCC 7420
AP009552.1	NCBI genome	*Microcystis aeruginosa* NIES-843
CP011304.1	NCBI genome	*Microcystis aeruginosa* NIES-2549
AM778951.1	NCBI genome	*Microcystis aeruginosa* PCC 7806
CP012375.1	NCBI genome	*Microcystis aeruginosa* NIES-2481
CP011339.1	NCBI genome	*Microcystis panniformis* FACHB-1757
CP001291.1	NCBI genome	*Cyanothece sp.* PCC 7424

Table 1: Strains and DNA sequences in this study, Continued

CP001344.1	NCBI genome	*Cyanothece sp.* PCC 7425
CP002198.1	NCBI genome	*Cyanothece sp.* PCC 7822
CP003646.1	NCBI genome	*Gloeocapsa* sp. PCC 7428
PRJNA46517	NCBI unassembled genome	*Gloeothece* sp. PCC 6909
CP003590.1	NCBI genome	*Pleurocapsa* sp. PCC 7327
CP002059.1	NCBI genome	*Nostoc Azollae* 0708
BA000019.2.1	NCBI genome	*Nostoc* sp. PCC 7120
AP017295.1	NCBI genome	*Nostoc* sp. NIES-3756
CP000117.1	NCBI genome	*Anabaena variabilis* ATCC 29413
CP003659.1	NCBI genome	*Anabaena cylindrica* PCC 7122
AJLN01000109.1	NCBI unassembled genome	*Chlorogloeopsis fritschii* PCC 6912
AJLM01000049.1	NCBI unassembled genome	*Chlorogloeopsis* sp. PCC 9212
ALWA01000002.1	NCBI unassembled genome	*Cyanobacterium* sp. PCC 7702
ALVU02000001.1	NCBI draft genome	*Synechocystis* sp PCC 7509
CP007542.1	NCBI genome	*Synechocystis* sp. PCC 6714
CP003265.1	NCBI genome	*Synechocystis* sp PCC 6803
This study	Sanger Sequencing and high throughput genome sequencing	*Synechocystis* sp WHSYN
This study	Sanger Sequencing 16s and phaC	*Synechocystis* sp LSNM3
This study	Sanger Sequencing 16s and phaC	*Synechocystis* sp CGF-1
This study	Sanger Sequencing 16s and phaC	*Phormidium*-like sp. *CGFILA*
This study and AY218830.2	NCBI and Sanger Sequencing 16s	*Phormidium autumnale* UTEX 1580 (*Cephalothrix komarekiana*)
This study	Sanger Sequencing 16s	*Oscillatoria Animalis* UTEX 1309
This study	Sanger Sequencing 16s	*Phormidium Fragilis* UTEX 2426
This study	Sanger Sequencing 16s	*Phormidium* cf. BC 1608
KJ994517.1	Sanger Sequencing 16s	*Phormidium Tergestinum* CCALA 155 (Cephalothrix komarekiana)
FN813343.1	Sanger Sequencing 16s	*Phormidium* cf. *Iriguum* CCALA 759
This study	Sanger Sequencing 16s	*Nodularia* sp. *Las Olas*
This study	Sanger Sequencing 16s	*Nodularia* sp. *WHNOD*
AY493588.1 AY493633.1	NCBI 16s, ITS	ULC 041 *Leptolyngbya* cf. *antarctica* ANT.ACE.1
This study	Work in progress	Sefil AB
KT753326.1	NCBI 16s	*Pseudanabaena frigida* ULC 066
KT753317.1	NCBI 16s	*Cyanobium* sp. *Bylot Island* ULC 065
KT753319.1	NCBI 16s	*Cyanobium* sp. *Laguna Chica* ULC 084
EU586733.1	NCBI 16s	*Nostoc Commune*
AY218827.2	NCBI 16s	*Nostoc Muscorum*

16s and 23s rRNA genes were aligned using the L-INS-i alignment method in MAFFT version 7.222. Coding DNA sequences were aligned according to standard codon translations via Muscle UPGMG clustering in MEGA version 7.0.21. Sequences were then imported into Mesquite version 3.20 for character tracing using Mesquite's most parsimonious reconstruction mode (MPRs mode), as well as for concatenation and reformatting of sequence files. For phylogenetic tree construction, JmodelTest version 2.17 was used to choose the best substitution model for each of the two datasets: 16s/23s rRNA, and phaE/phaC PHA synthase genes. The GTR+I+G substitution model was found to be most appropriate. Maximum likelihood phylogenetic trees were then constructed for each dataset using a partitioned maximum likelihood analysis, with 100 rapid bootstrap replicates in RaxML GUI version 1.5. The purple sulfur bacterium *Thioalkalivibrio sulfidophilus* HL-EbGr7 was selected as an outgroup because it belongs to a clade of purple sulfur bacteria containing two-component PHA synthase genes similar to those of cyanobacteria.

Two programs, originally designed to analyze host and parasite co-phylogenies were then used to compare 16s/23s phylogenies with PHA synthase gene phylogenies. For each of these programs, the 16s/23s tree was specified as the independent "host" tree, and the phaE/phaC tree was specified as the dependent "parasite" tree. The first program, Tree Map 3, uses a heuristic algorithm which "untangles" the dependent and independent trees, aligning them in a way which

most clearly illustrates any incongruences between the two phylogenies (79). The second program, Jane (version 4), uses genetic and dynamic timing algorithms designed to identify models of co-evolution which optimally account for the similarities and incongruences between two phylogenies according to a cost-minimizing scheme (80). The default cost values used in the Jane analysis are listed in table 2. In general, solutions with a lower overall cost are considered to be more plausible models of co-evolution than solutions with higher cost.

Table 2: Jane (version 4) default cost values used in this study

Event	Cost
Cospeciation	0
Duplication	1
Loss	1
Failure to Diverge	1
Duplication + Host Switch	2

The Jane model parameters were set to a population of 500 for 250 generations. For the purposes of this study, a duplication + host switch event was considered to be analogous to a horizontal gene transfer event.

2. Culture Conditions

Nile Red and boron-dipyrromethene (BODIPY) 493/503 screenings were conducted in replicate 25 ml cultures grown in 50ml test tubes, in F/2 or BG11 media under constant light. Initial screenings were performed during exponential and stationary phases under nitrogen-rich and nitrogen-limited conditions. Further screening of *Nodularia* sp. *Las Olas* was performed using the same conditions described above, in F/2 media with varying nitrate, ammonia, phosphate, and salt

concentrations. Chla fluorescence was measured to track growth, using a Turner Designs 10AU fluorometer.

Osmotic shock experiments were performed by centrifuging stationary phase cultures at 1000 xg for 10 minutes, and re-suspending the resulting pellet either in seawater that had been diluted with MilliQ ultrapure water, or seawater that had been spiked with sea salt.

Chemical analyses were performed on cell pellets of axenic 1L cultures, grown in 3L flasks under constant light and stirring, and harvested in early stationary phase, 25-30 days since inoculation. Chla fluorescence was monitored using a Turner Designs AquaFluor handheld fluorometer. Cells were harvested via centrifugation for 20 minutes at 8326 x g. For FTIR and HPLC, salts were removed by washing cell pellets twice with an equivalent volume of either 0.5M or 0.75M ammonium carbonate for cultures grown at ≤35% salinity, or >35% salinity, respectively. Wet biomass pellets were frozen and stored at -80°C. Dry biomass pellets were lyophilized at -80°C for two days, then stored in a desiccator at room temperature.

3. Staining and Counting of Granules

Nile Red and BODIPY 493/503 are lipophilic dyes that fluoresce in hydrophobic environments. As a result, they are commonly used for *in situ* screening of algae as biofuel and bioproduct feedstocks (13, 14).

Staining was performed on 500ul aliquots taken from each sample after thorough mixing. 1 ul of 0.1 mg/ml BODPIPY or Nile Red stock was added to each aliquot, vortexed thoroughly, then incubated in the dark for 15 minutes. Samples were then imaged at 400x and 1000x magnification in a fluorescent microscope with an 89 North Fluorophore light source. Images were taken using a SPOT Pursuit camera and software system (version 5.0) under RGB fluorescence. Staining granules were counted from three different sections of each slide, consisting of at least five cells from each filament and at least one hundred cells in total.

4. Proton NMR

PHB ^{1}H NMR was performed using methods descried by Linton et al. in 2012 (81). Eighteen milligrams of lyophilized cell pellets from staining cultures, the non-staining strain *Nodularia* sp. *WHNOD*, and purified poly(R)-3 hydroxybutyric acid from Sigma Aldrich were suspended in 1 mL of $CDCl_3$ and 58l µl sodium hypochlorite. The suspensions were vortexed thoroughly for 10 minutes, then incubated in an agitator for two hours at 30°C. Phase separation was induced by centrifuging the suspensions at 1,500 xg for 10 minutes, after which the bottom organic phase was removed using a syringe. ^{1}H NMR was performed on 500 µl organic extracts from each sample, using a Varian Mercury Plus 400 MHz spectrometer and 5mm NMR tubes. H_1 NMR data were processed using MestreNova software.

5. FTIR

FTIR was performed using methods described by Levering et al. in 2016 (82). Lyophilized biomass pellets of *Nodularia* sp. *Las Olas* were crushed with a chemical spatula and packed into a Shimazu IRprestige-21 spectrophotometer with single reflection ATR from PIKE Technologies. Biomass was added to the spectrophotometer well until signal saturation. Each spectrum measurement was the average result of 20 readings, and three measurements were taken for each sample.

6. Lipid Analysis

An Agilent Technologies 7890A GC system, coupled with an Agilent Technologies 5975C VL MSD with Triple-Axis Detector were used to analyze lipid extracts from the non-staining strains *Phormidium autumnale* UTEX 1580, and *Nodularia* sp. *WHNOD*, as well as the staining strains *Phormidium* cf. *Iriguum* CCALA 759 and *Nodularia* sp. *Las Olas.*

Lipids were extracted from 30 mg of lyophilized biomass using a scaled-down protocol adapted from Schoepp et al. (83). 30mg of biomass was suspended in 390 µl isopropanol and 330 µl hexane for one hour at 45 °C. The suspension was then centrifuged at 21130 xg for 10 minutes, and the hydrophobic layer was removed. Raw hexane extracts were then stored at -80°C. An additional pair of biological replicates was also prepared for *Nodularia* sp. *Las Olas* grown at 10% and

150% salinity using the same method described above, extracted with 500ul instead of 330 µl hexane.

Total lipid profiles were obtained by suspending 20 µl of raw hexane extract in 1 mL 1M HCl in methanol at 60°C for 30 minutes, and extracted once again with 1 mL hexane. The esterified extracts were analyzed via GC-MS, after the addition of a C19 methyl ester standard, to the final concentration of 5.1 ug/ml.

Raw hexane extracts were also spotted on a TLC plate. Vegetable oil was diluted 1:50 in hexanes and spotted as a standard. Two solvent systems were used to develop the plates. The first solvent system consisted of acetone:toluene:H_2O in a 91:30:3 ratio, and it was allowed to run two-thirds of the length of each TLC plate. After air-drying, the TLC plates were then transferred into a jar containing the second solvent system. The second solvent system consisted of hexanes/diethylether/acetic acid in a 17:3:0.2 ratio, and it was allowed to run the complete length of the plate. This two-solvent system separates polar lipids from neutral lipids. TLC plates were then broken in half. Half of the plate was developed in a solution containing 20g $CuSO_4$, 8ml H_2SO_4, and 8ml H_3PO_4, and charred at 120 °C. Based on the Rf values from the charred half of the TLC plate, spots were scraped off the other, un-charred half into 1mL 1M HCl in methanol, and esterified using the same protocol as before. The esterified extracts were analyzed via GC-MS.

7. Purification of CGP-like granules in *Nodularia* sp. Las Olas

A modified version of the CGP extraction protocol described by Robert Simon

in 1973 (84) was used to determine whether the increased arginine composition of staining *Nodularia* sp. *Las Olas* cultures could be attributed to the presence of a CGP-like granule. 25ml of staining and non-staining stationary phase cultures of *Nodularia* sp. *Las Olas*, along with 25ml of *Anabaena* sp. strain PCC 7120 were pelleted at 8326 xg for 20 minutes. The cell pellets were then re-suspended in 2ml milliQ water and passed through a French press three times at 1120 psi. The lysed cell suspensions were then centrifuged at 27,000 xg for 15 minutes, and the supernatant fluid was removed. The cell pellet was then washed sequentially with MilliQ water, 2% Triton-X 100, and an additional two washes of MilliQ water. After the final wash, the pellet was extracted twice with 1ml 0.1 N HCl for 30 minutes. Extracts and pellets from each purification step were stored at -80°C.

8. HPLC Amino Acid Analysis

Amino acid analysis of lyophilized cell pellets was performed using a modified version of the HPLC protocol described by Broek and McCarthy, 2014 (85). Lyophilized cell pellets and CGP-like granule extracts were hydrolyzed with 6M HCl at 90°C for 24 hours, then dried using a centrifugal evaporator at 60°C. Samples were then re-dissolved in 0.1 N HCl, filtered through 0.2 um PTFE filters, dried once again, and redissolved in MilliQ water with 0.1% Trifluoroacetic acid (Solvent A). Lyophilized samples were stored in a dessicator before hydrolysis, and at -80°C after hydrolysis. HPCL was performed using an agilent technologies 1200 series

liquid chromatograph with a 385-ELSD evaporative light scattering detector, and a SiELC Primesep A column (10 × 250 mm, 100 Å pore size, 5 µm particle size; SiELC Technologies Ltd.)

Additional amino acid analyses of lysed and washed cell pellets were performed on a biological replicate at the UC Davis molecular structure facility using a similar protocol. Samples were hydrolyzed at 6M HCl at 110°C for 24 hours, and loaded onto a Hitachi L-8800 analyzer using a sodium citrate buffer system

Results

1. Screening of Cyanobacteria for PHA and other Hydrophobic Granules

Twenty cyanobacteria were stained with Nile Red and BODIPY 493/503 and screened for phaC via PCR (Table 3). Staining and PCR amplification of phaC in the model strain *Synechocystis* sp. PCC 6803 was used to verify the screening methods of the study. Most of the cyanobacteria that did accumulate staining granules also possessed a phaC polyhydroxyalkanoate synthase gene. There were, however two exceptions: *Phormidium* cf. *iriguum* CCALA 759, and the strain *Nodularia* sp. *Las Olas*. These two strains did accumulate staining granules, but did not seem to possess a phaC gene. Notably, the polar-adapted strain *Nostoc* cf. *muscorum* did not produce PHB granules despite the fact that PHB accumulation is well documented in other strains of *Nostoc muscorum*. Figure 1 shows images of representative positive granule accumulating strains.

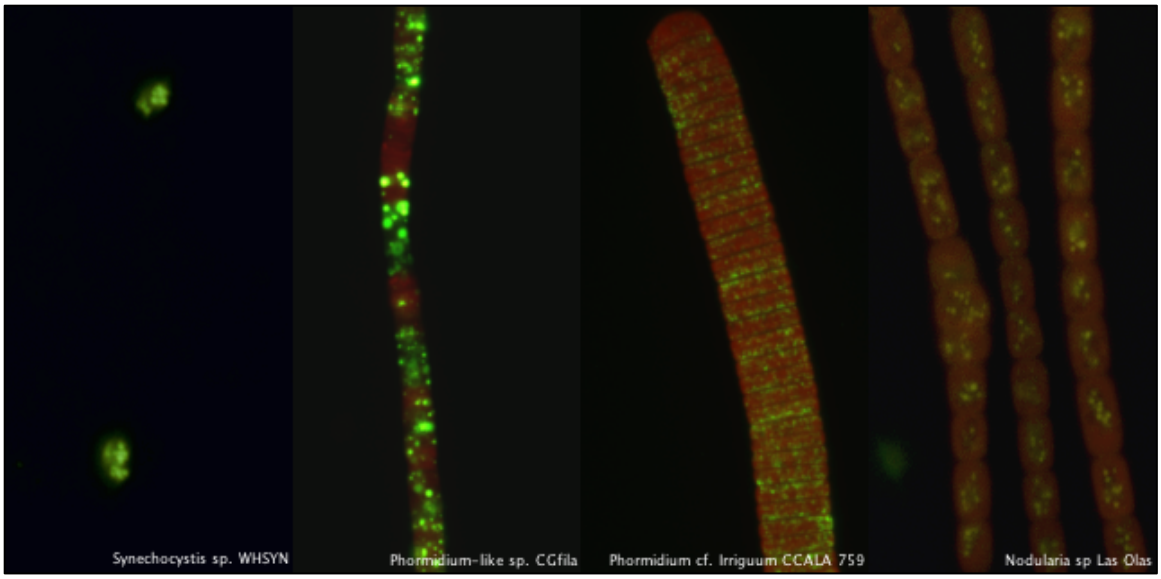

Figure 1: Bodipy 493/503 staining of representative cyanobacteria strains. Staining granules appear green, whereas chlorophyll autofluorescence appears red.

Table 3: Summary of PhaC Screening Results

Name of strain	BODIPY 493/503 staining	Nile Red staining	PhaC PCR screening
Synechocystis sp. PCC 6803	+	+	+
Synechocystis sp. *WHSYN*	+	+	+
Synechocystis sp. *LSNM3*	+	+	+
Synechocystis sp. *CGF*-1	+	+	+
Phormidium sp. *CGFILA*	+	+	+
Phormidium autumnale UTEX 1580 (Cephalothrix komarekiana)	-	-	-
Oscillatoria Animalis UTEX 1309	-	-	-
Phormidium Fragilis UTEX 2426	-	-	-
Phormidium Tergestinum CCALA 155 (*Cephalothrix komarekiana*)	-	-	-
Phormidium cf. *Iriguum* CCALA 759	+	+	-
Nodularia sp. *Las Olas*	+	+	-
Nodularia sp. *WHNOD*	-	-	-
Leptolyngbya cf. *antarctica* ANT.ACE.1 ULC 041	-	-	-
Sefil AB	-	-	-
Pseudanabaena frigida ULC0 66	-	-	-
Cyanobium sp. ULC 84	-	-	-
Cyanobium sp. O-154 ULC 65	-	-	-
Nostoc cf. Commune	-	-	-
Nostoc cf. *Muscorum*	-	-	-
Phormidium cf. BC 1608	-	-	-

2. ^{1}H NMR Spectroscopy of Staining Strains

^{1}H NMR was then performed on hydrophobic extracts of these representative strains (see Materials and Methods). Extracts from *Synechocystis* sp. *WHSYN* and *Phormidium*-like sp. *CGFILA* were both found to produce Poly-3-hydroxyutryate, the most common PHA found in cyanobacteria (Figure 2). This verifies that the staining strains which possess phaC genes are also producing polyhydroxyalkanoates.

Conversely, the ^{1}H NMR spectra of extracts of the staining, but phaC-negative strains *Phormidium* cf. *iriguum* CCALA 759 and *Nodularia* sp. *Las Olas* did not contain peaks consistent with those PHB (Figure 2). Although cyanobacteria can produce non-PHB polyhydroxyalkanoates, these PHAs are only known to be produced alongside PHB (21, 23, 24). Thus, these two strains do not produce PHAs under the conditions tested here.

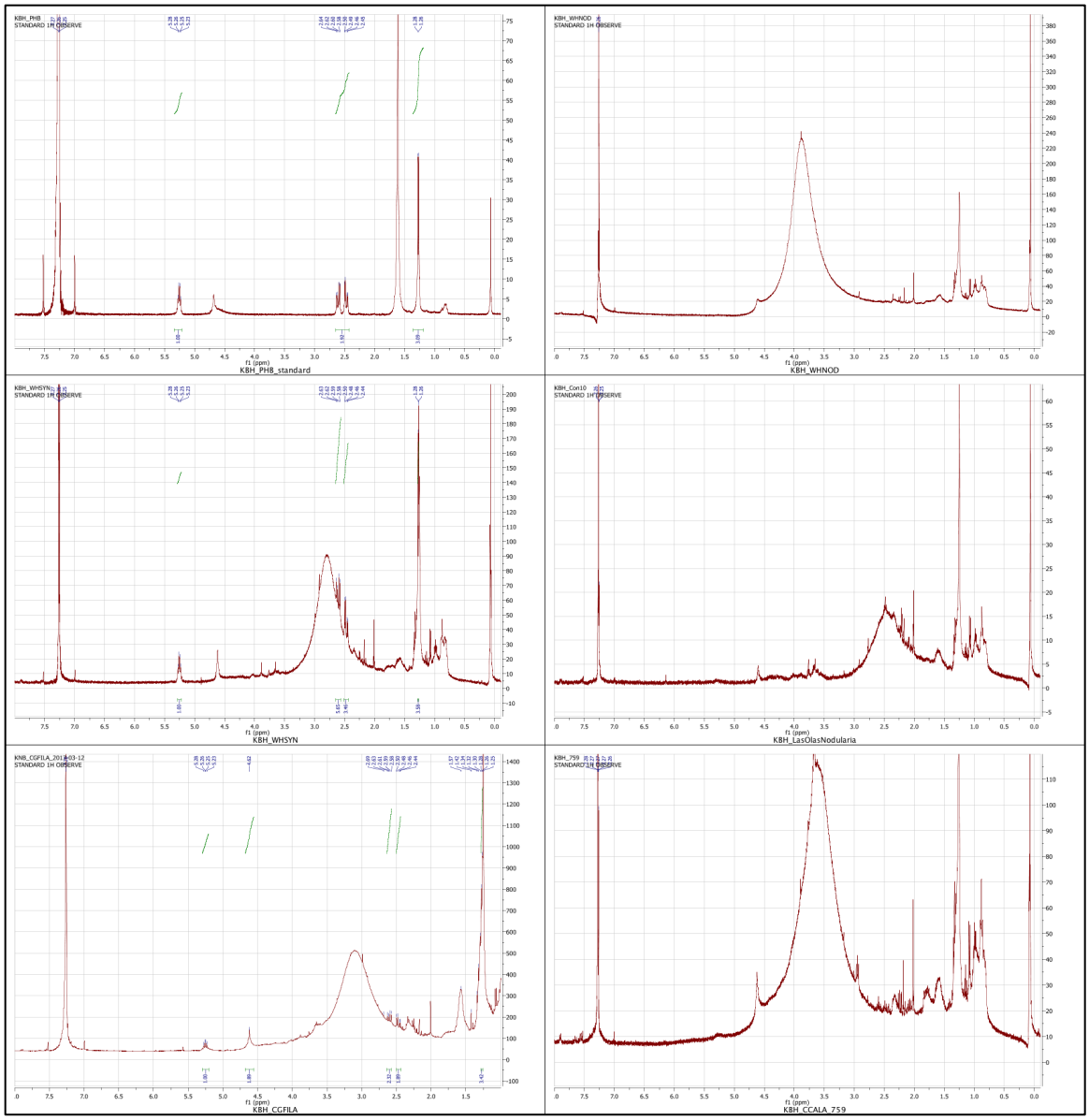

Figure 2: ^{1}H NMR of hydrophobic extracts from representative cyanobacteria strains. The non-staining, phaC negative strain *Nodularia* sp. WHNOD was analyzed as a negative control. Purified PHB was analyzed as a standard. The X-axis shows chemical shifts in parts per million (ppm). The Y-axis shows normalized relative intensity values. Peaks at chemical shifts consistent with those of the PHB standard are marked and labeled with integration values, which are representative of the relative number of hydrogen atoms present in each chemical environment.

3. Phylogenetic Analysis of Polyhydroxyalkanoate Synthase Gene phaC

3.1 Contextualizing Screening Results with 16s and 23s rRNA Phlogeny

In order to contextualize the significance of these results, a 16s and 23s ribosomal RNA phylogeny of available cyanobacterial sequences was constructed and the character history of PHA biosynthesis was traced via maximum parsimony reconstruction. The occurrence of PHB biosynthesis in the recently isolated strains *Synechocystis* spp. *WHSYN*, *LSNM*, and the freshwater strain *CGF-1* is consistent with the occurrence of PHA accumulation by *Synechocystis* spp. PCC 6803 and PCC 6714. Indeed, PHA biosynthesis is very well-conserved within the genus *Synechocystis*, even among freshwater strains like S*ynechocystis* sp. *CGF-1* (Figure 3).

Furthermore, the dye-staining strains *Nodularia* sp. *Las Olas* and *Phormidum* cf. *irriguum* CCALA 759, which do not synthesize polyhydroxyalkanoates based on *phaC* PCR screening and H_1 NMR spectroscopy, both belong to phylogenetic clades characterized by widespread PHA synthase gene loss (Figure 3).

On the other hand, *Phormidium-like* sp. *CGFILA* is also located within an island of PHA synthase gene loss; however, PCR screening, and ^1H NMR analysis show that CGFILA does accumulate PHB. This can be explained either by the loss of PHA biosynthesis among many *Phormidi*um strains or a case of horizontal gene transfer into the genome of a recent ancestor of *Phormidium*-like sp. *CGFILA*.

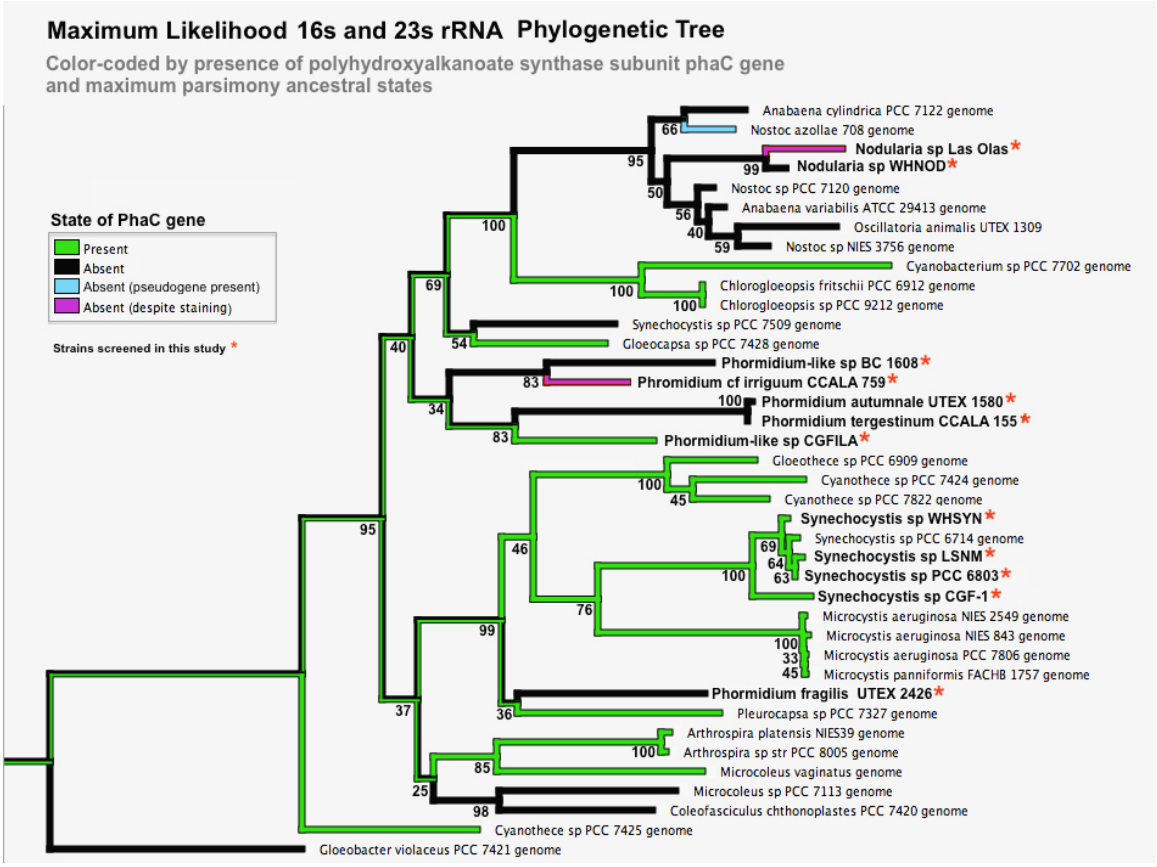

Figure 3: a maximum likelihood phylogeny of cyanobacterial 16s and 23s rRNA genes. Bootstrap values are indicated at each node.

3.2 Genetic Survey of PHA Biosynthesis Operons

The PHA biosynthesis operons present in 23 cyanobacteria genomes were also examined. The relative locations and orientations of these operons were found to vary greatly, even between closely related cyanobacteria strains. Nevertheless, a few meaningful observations could be made. In general, *phaE* is typically transcribed before *phaC*, and *phaA* is typically transcribed before *phaB* (Table 4). When the four genes are split between two different operons, *phaA* is almost always on the same operon as *phaB*, and *phaE* is almost always on the same operon as *phaC* (Table 4). Few exceptions to this rule were observed. The organisms in which *phaA* is encoded separately from *phaB* all belong to same monophyletic clade containing

Chlorogloeopsis fritschii PCC 6912, *Chlorogloeopsis* sp. PCC 9212, and Cyanobacterium sp. PCC 7702. The other exception to this rule belongs to the symbiont *Nostoc azollae* 708, which appears to have lost its *phaE* gene. The *phaC* and *phaB* genes of *Nostoc azollae* 708 are also frame shifted, and there are internal stop codons present in the genes *phaC*, *phaA*, and *phaB*. This suggests that the PHA biosynthesis genes of *Nostoc azollae* 708 are no longer functional, and its missing *phaE* gene is most likely explained by one or more deletion mutations. This would represent a likely relatively recent loss of PHA synthesis.

Table 4: PHA Biosynthesis operon topology

Name of strain	Operon Topology		
Thioalkalivibrio sulfidophilus HL-EbGr7	single	<--CE--< >--AB-->	
Arthrospira sp. PCC 8005	split	>--EC-->	<--BA--<
Arthrospira platensis NIES39	split	>--AB-->	<--CE--<
Arthrospira platensis YZ	split	>--AB-->	<--CE--<
Microcoleus vaginatus	split	>--EC-->	<--BA--<
Microcystis aeruginosa NIES-843	single	<--CEBA--<	
Microcystis aeruginosa NIES-2549	single	<--CEBA--<	
Microcystis aeruginosa PCC 7806	single	>--ABEC-->	
Microcystis aeruginosa NIES-2481	single	<--CEBA--<	
Microcystis panniformis FACHB-1757	single	<--CEBA--<	
Cyanothece sp. PCC 7424	single	>--ABEC-->	
Cyanothece sp. PCC 7425	single	>--ABEC-->	
Cyanothece sp. PCC 7822	single	>--AB-transposase-EC-->	
Gloeocapsa sp. PCC 7428	single	>--ECAB-->	
Gloeothece sp. PCC 6909	single	>--C--> <--EBA--<	
Pleurocapsa sp. PCC 7327	split	>--AB-->	>--EC-->
Nostoc Azollae 0708	Single	>--C-transposases-AB-->	
Chlorogloeopsis fritschii PCC 6912	split-A	>--BEC-->	>--A-->
Chlorogloeopsis sp. PCC 9212	split-A	<--A--<	<--CEB--<
Cyanobacterium PCC 7702	split-A	<--CEB--<	<--A--<
Synechocystis sp. PCC 6714	split	<--BA--<	<--CE--<
Synechocystis sp. PCC 6803	split	>--AB-->	>--EC-->
Synechocystis sp *WHSYN*	split	<--BA--<	>--EC-->

3.3 Cophylogenetic Analysis of *phaE/phaC* and 16s/23s rRNA Phylogenies

A joint phylogenetic analysis of the PHA synthase genes *phaE* and *phaC* genes was then performed. The decision to include sequences of *phaE*, when available, with those of *phaC* was made because *phaE* and *phaC* are almost always transcribed together in cyanobacteria (Table 3), each coding for a monomeric component of the same heterodimer PHA synthase protein. This joint *phaC* and *phaE* phylogeny was then compared with a joint 16s and 23s rRNA phylogeny in order to determine whether the two phylogenies are congruent (Figure 4A). No evidence of horizontal gene transfer between cyanobacteria and non-cyanobacterial eubacteria was found. Furthermore, the 16s/23s rRNA and *phaC*/*phaE* phylogenies were generally congruent, with the exceptions of *Pleurocapsa* sp. PCC 7327. Although *Pleurocapsa* sp. PCC 7327 is sister to the clade containing *Cyanothece* spp. PCC 7424 and PCC 7822 according to the 16s and 23s rRNA phylogeny, its phaC and phaE genes are most closely related to those of *Phormidium*-like sp. *CGFILA*. This incongruence is supported by nodes with bootstrap values of 94 and 68 for the 16s/23s rRNA and phaC/phaE phylogenies, respectively (Figures 4b and 4c).

Other incongruences occurred at nodes with lesser or no bootstrap support. *Microcoleus vaginatus* FGP-2 also appears to have incongruent 16s/23s rRNA and PHA synthase phylogenies; however, the rooting of the PHA synthase phylogeny precludes support at the critical node. Additionally, the *phaC* and *phaE* phylogenies of genus S*ynechocystis* are more similar to those of *Arthrospira* than they are to *Microcystis*, despite *Synechocystis* being more closely related to *Microcystis* based on

16s and 23s rRNA. This incongruence is supported by nodes with bootstrap values of 78 and 45 for the 16s/23s rRNA and phaC/phaE trees, respectively (Figures 4B and 4C).

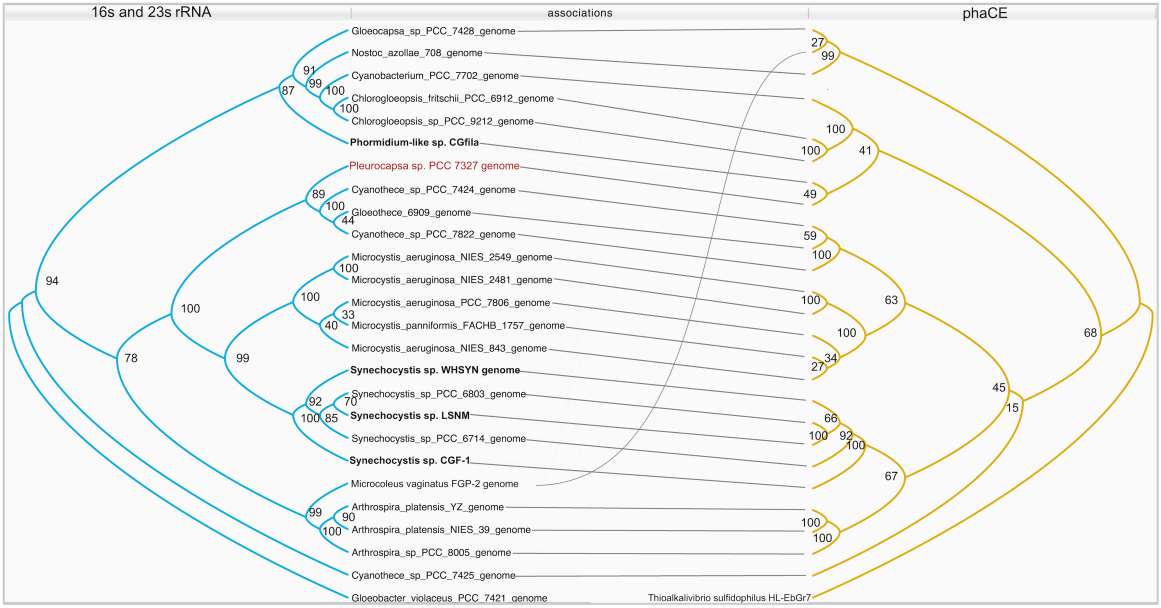

Figure 4a: TreeMap co-phylogeny of maximum likelihood 16s/23s rRNA and *phaC/phaE* gene trees. Bootstrap values are indicated at each node. PHB producers characterized in this study are in bold, and strains with incongruent phylogenies are indicated by red text.

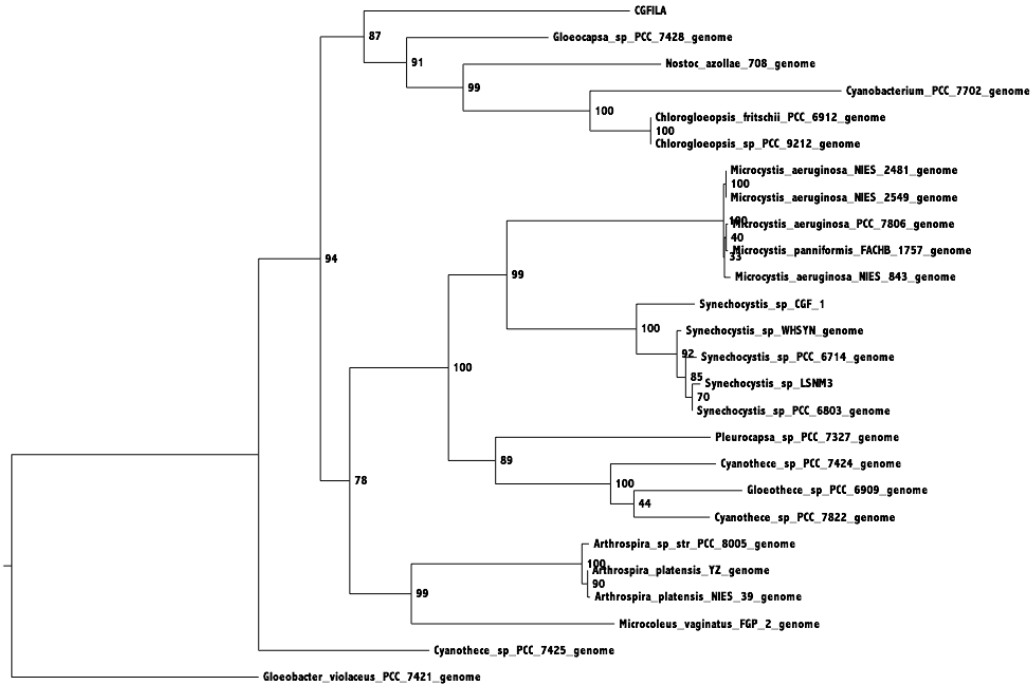

Figure 4b: Maximum likelihood 16s and 23s rRNA gene tree of cyanobacteria with *phaC* genes. This tree was used to construct Figure 4a.

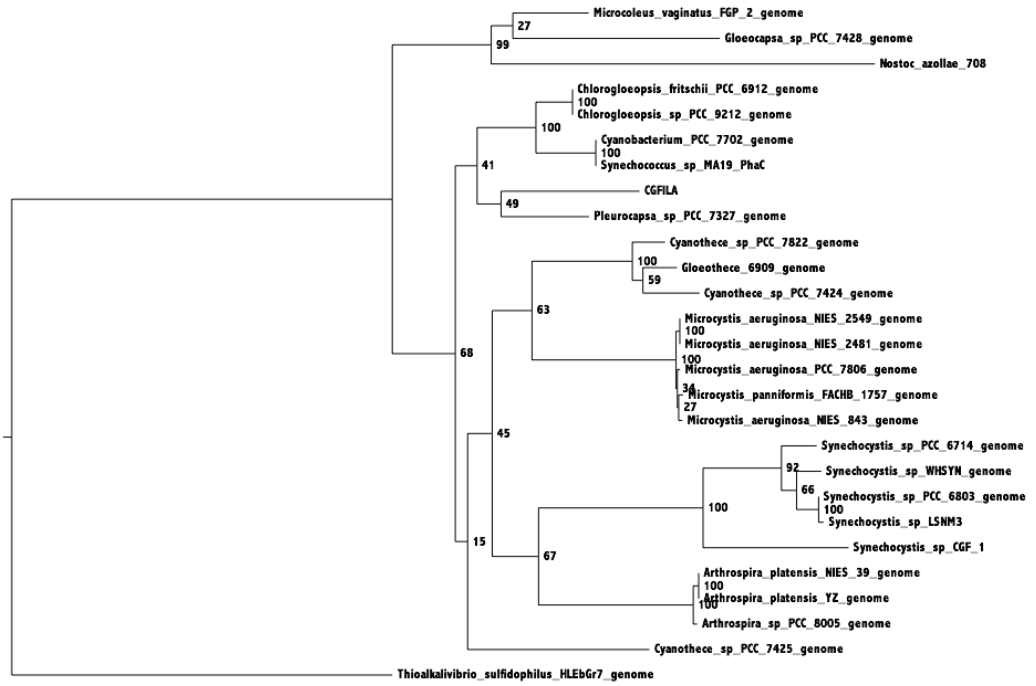

Figure 4c: Maximum likelihood cyanobacterial *phaC* and *phaE* gene tree used to construct Figure 4a.

Jane, an evolutionary modeling program, was then used to find the most parsimonious co-phylogenetic reconstructions that account for the incongruences between the 16s/23s and *phaC*/*phaE* phylogenies described above. The heuristic search yielded four equally parsimonious solutions, all with a cost of 25 (Figure 5). A random sampling of 100 solutions to this co-phylogenetic reconstruction problem contained solutions with a mean cost of 41.99 and a standard deviation of 1.92. Thus, the four solutions of cost 25 were not only the solutions of lowest cost, but were also of significantly lower cost than other solutions to the co-phylogenetic reconstruction problem, indicating that these solutions are significantly more parsimonious than other co-phylogenetic reconstructions. A histogram of these randomly sampled solutions is shown in Figure 5. All four of these most-parsimonious solutions propose that one or more horizontal gene transfer (duplication + host switch) events have occurred between recent ancestors of the strains, *Pleurocapsa* sp. PCC 7327 and the novel *Phormidium*-like sp. *CGFILA* (Figure 5). The four solutions also propose instances of horizontal gene transfer of PhaC between ancestors of *Microcoleus vaginatus* FGP-2 and *Gloeocapsa* sp. PCC 7428, as well as between the ancestors of the genera *Synechocystis* and *Arthrospira* (Figure 5). However, it is important to note that Jane analyses only propose mechanisms of evolution given specific phylogenies; thus, a proposed evolutionary event is only as well-supported as the participating nodes of the underlying phylogenies, presented in Figures 4b and 4c.

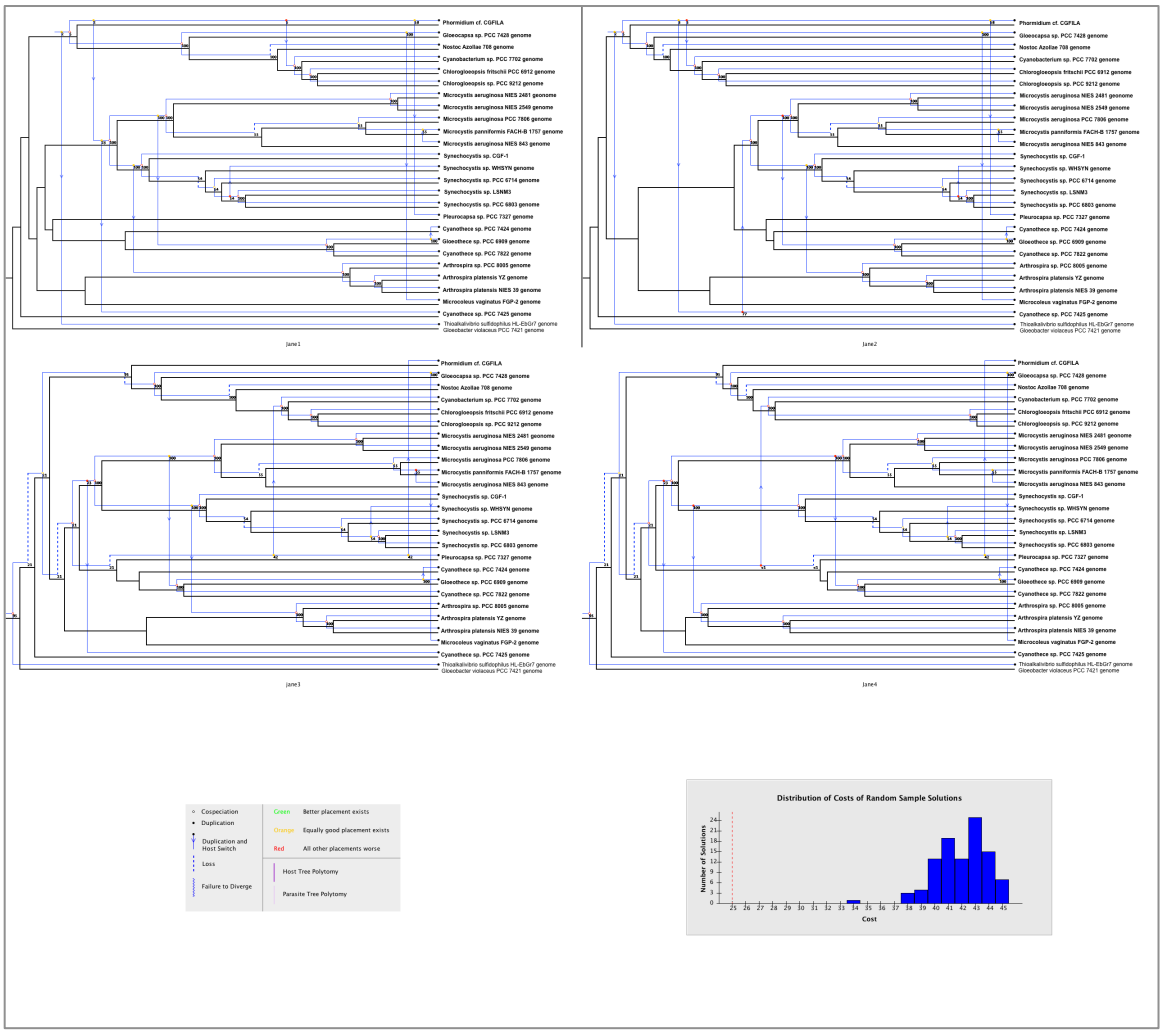

Figure 5: The four best co-phylogenetic reconstructions of the given cyanobacteria 16s/23s and phaE/phaC trees according to JANE (top). A legend, as well as a distribution of costs for a random sample of solutions is also shown (bottom)

4. Accumulation and Degradation of Granules in *Nodularia* sp. *Las Olas*

4.1 Effects of Salinity on Accumulation and Degradation of Granules

In order to better understand the staining granules of *Nodularia* sp. *Las Olas*, granules per cell were counted for cultures grown under nitrogen limitation, phosphate limitation, light limitation, and osmotic stress conditions.

Osmotic stress has a significant effect on granule production. When quadruplicate cultures of *Nodularia* sp. *Las Olas* were grown at 10%, 50%, and 100% salinity relative to seawater, more granules per cell were observed in cultures grown at lower salinities when compared to cultures grown at higher salinities. At stationary phase, 3.45 +/- 0.21 ($\bar{x}$ +/- σ) granules per cell were observed in cultures grown at 10% the salinity of seawater, compared to 1.93 +/- 0.40 granules per cell in cultures grown at 50% salinity, and 1.20 +/- .07 granules per cell in cultures grown at 100% salinity (Figure 6a). Additional experiments show that cultures of *Nodularia* sp. *Las Olas* grown in F/2 media at 150% salinity produce very few granules per cell (Figure 6b).

Furthermore, salt-shocking stationary phase cultures of *Nodularia* sp. Las Olas grown at 10% salinity leads to the degradation of staining granules. When cultures grown in F/2 media at 10% the salinity of seawater were re-suspended with seawater diluted to 10%, 50% and 75% salinity, a sharp decrease in the number of granules per cell was observed in the salt-shocked cultures, but not in the control group (Figure 7).

Thus, *Nodularia* sp. *Las Olas* accumulates more staining granules per cell at low salinity than at higher salinities, and these granules are degraded when cultures are moved from low salinity to higher salinities in the absence of cell growth.

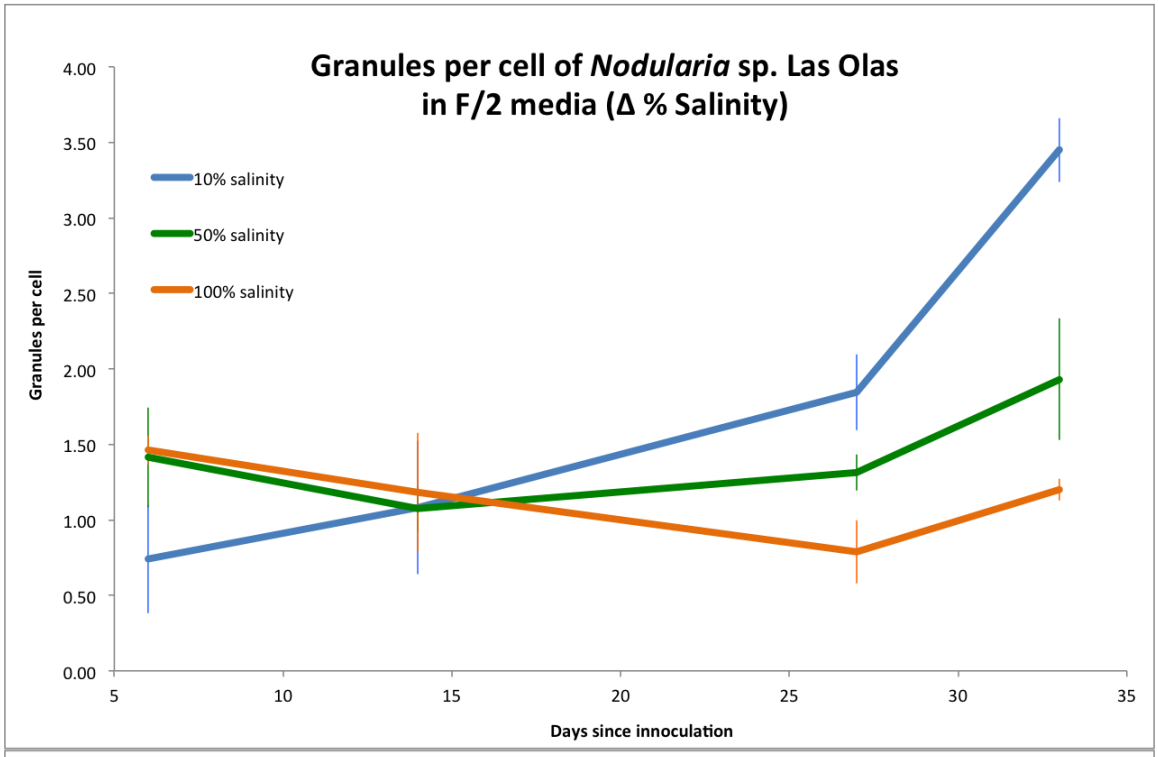

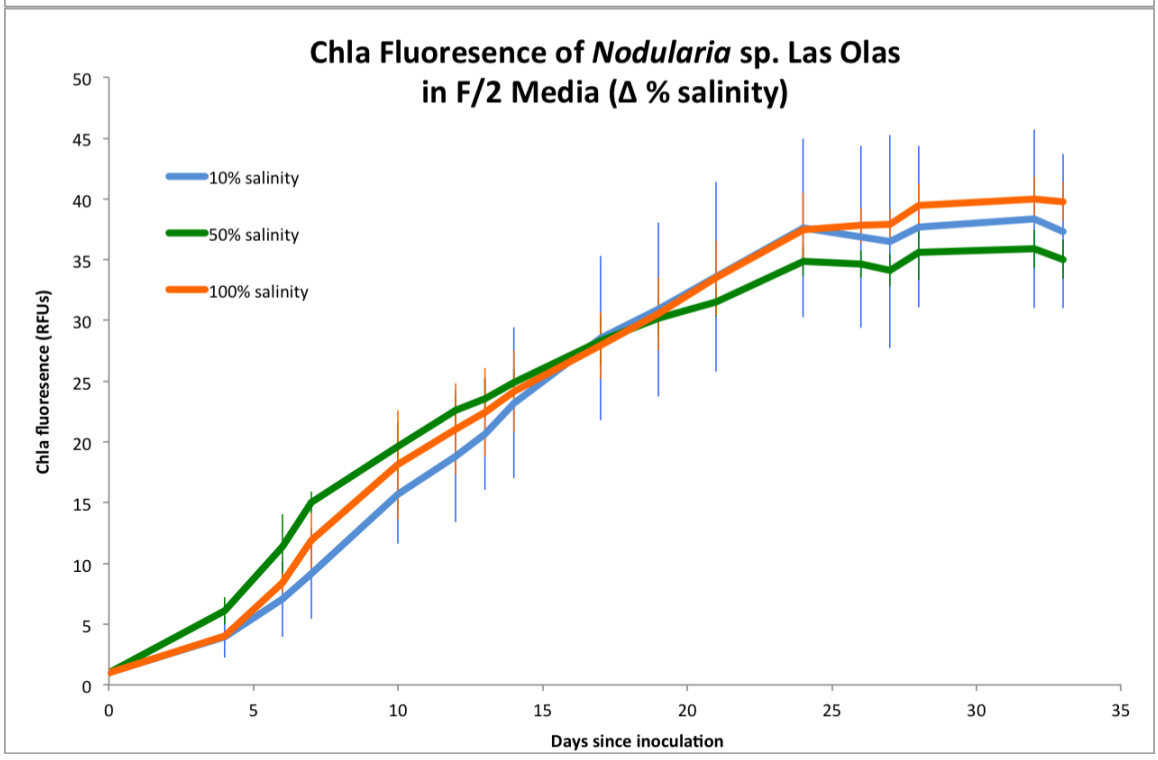

Figure 6a: Granules per cell of *Nodularia* sp. Las Olas grown in F/2 media with variable salinity. Data shown are averages from four replicates. Error bars show 95 percent confidence intervals. Chla fluorescence of said cultures are included as a measurement of growth.

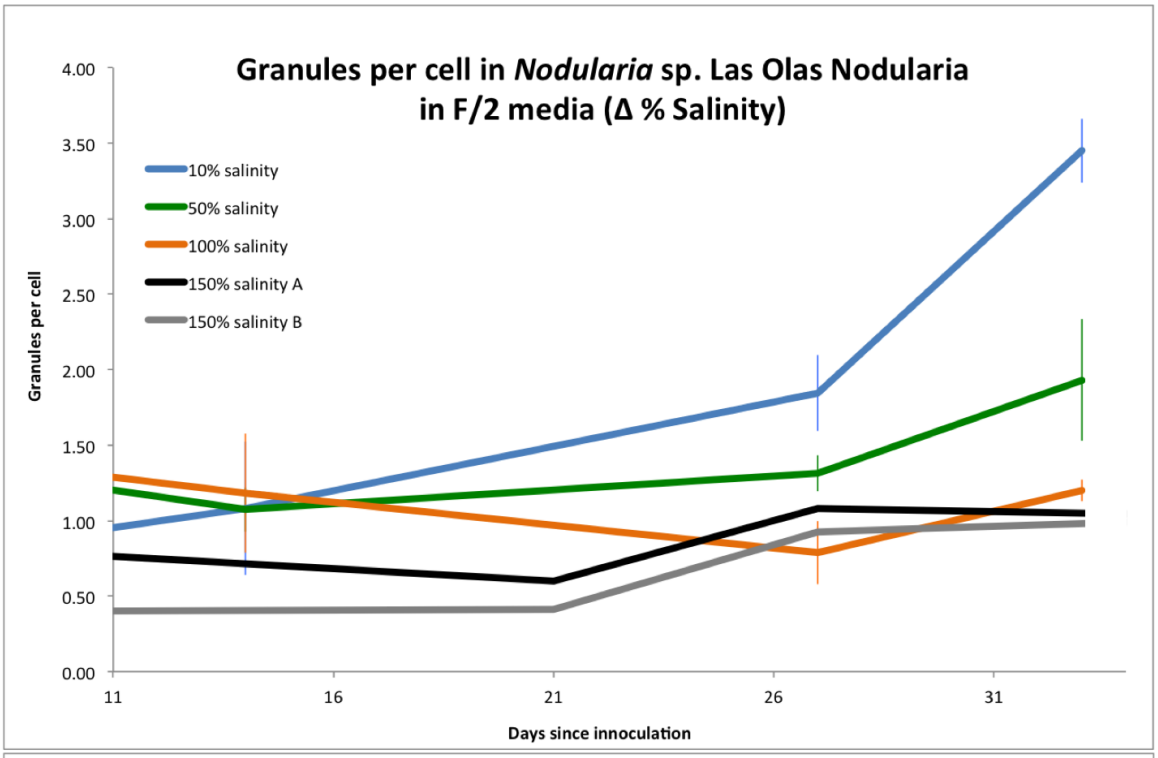

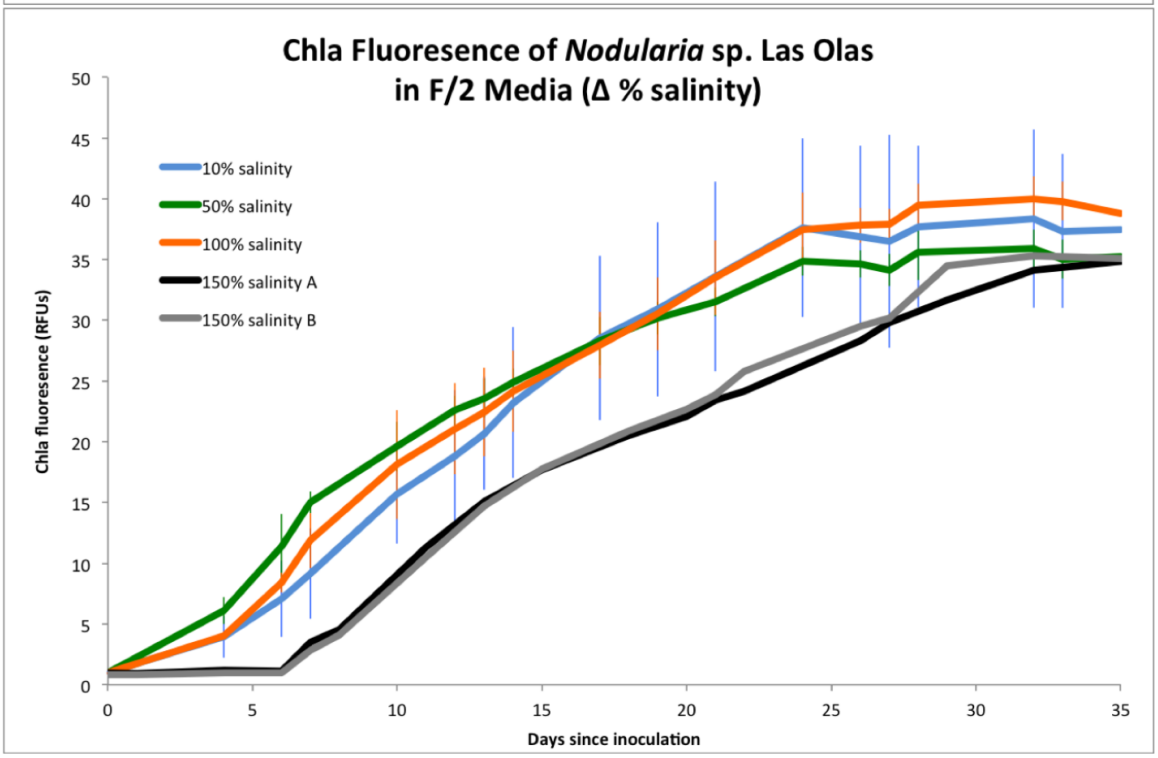

Figure 6b: Granules per cell of *Nodularia* sp. Las Olas grown in F/2 media with variable salinity, including an additional pair of cultures grown at 150% salinity using Red Sea salts. Both replicates are shown. All other data are averages from four replicates. Error bars show 95 percent confidence intervals. Chla fluorescence of said cultures are included as a measurement of growth.

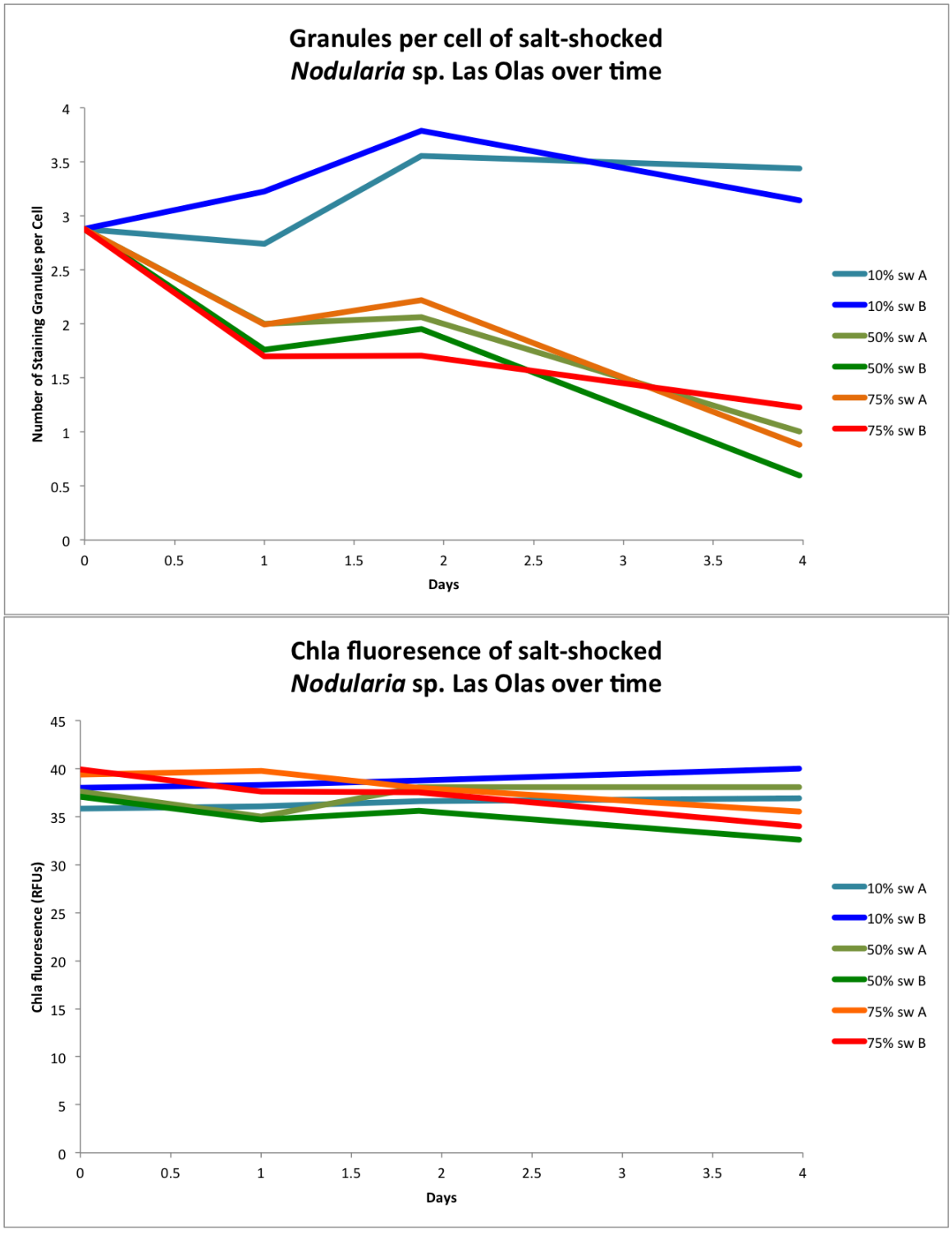

Figure 7: Degradation of staining granules under salt shock conditions by *Nodularia* sp. Las Olas. Two replicates for each treatment are shown.

4.2 Effects of Nitrogen and Phosphate Limitation on Accumulation of Granules

The highest accumulation of staining granules in *Nodularia* sp. *Las Olas* were observed during stationary phase, as shown in Figure 6. Cultures of *N.* sp. *Las Olas* were then grown under phosphate and nitrogen limitation in order to determine whether the presence of phosphate and/or nitrogen plays a regulatory role in granule accumulation.

When *N.* sp. Las Olas was grown in F/2 media supplied with three different concentrations of $NaH_2PO_4 \bullet 2H_2O$, stationary phase cultures grown at lower phosphate concentrations accumulated more granules per cell than cultures grown at higher phosphate concentrations. This suggests that phosphate limitation plays a role in inducing granule accumulation (Figure 8).

Unlike phosphate limitation, nitrogen status did not have discernable effect on granule accumulation (Figure 9). This was true for nitrogen fixing cells, cultures provided with nitrate,and cultures provided with ammonia.

4.3 Effect of Light Limitation on Accumulation of Granules

Granule accumulation increased slightly under light deprivation. Cultures of *Nodularia* sp. *Las Olas* grown under constant light at 100% salinity accumulated an average of 0.62 +/- 0.31 granules at 22 days post-inoculation. Identical cultures of *Nodularia* sp. *Las Olas* which had been placed in the dark at day 13 accumulated 1.25 +/- 0.28 granules 8 days later (day 22), after which the cultures began to die (Figure 10).

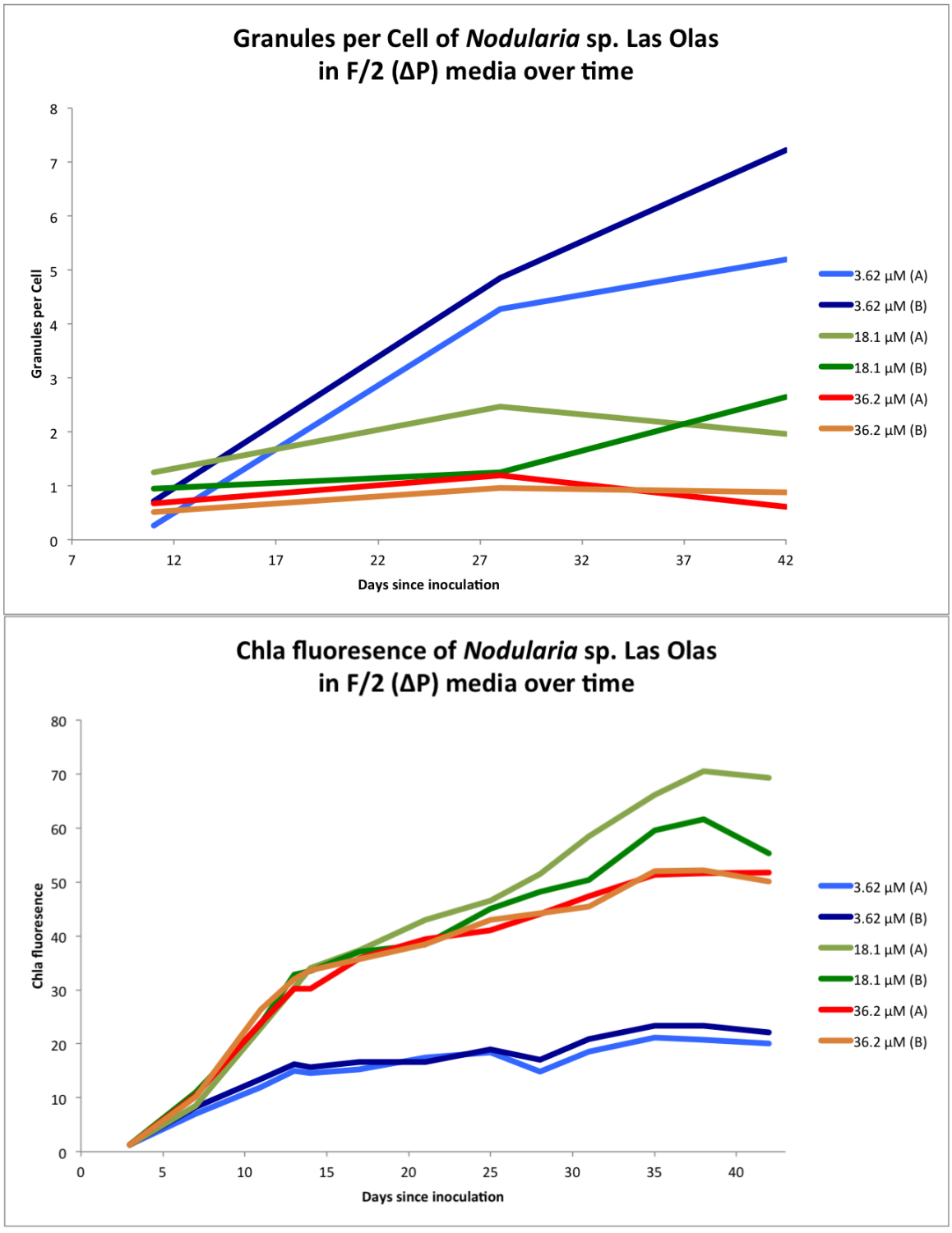

Figure 8: Granules per cell and Chla fluorescence of *Nodularia* sp. Las Olas over time. Two replicates for each treatment are shown.

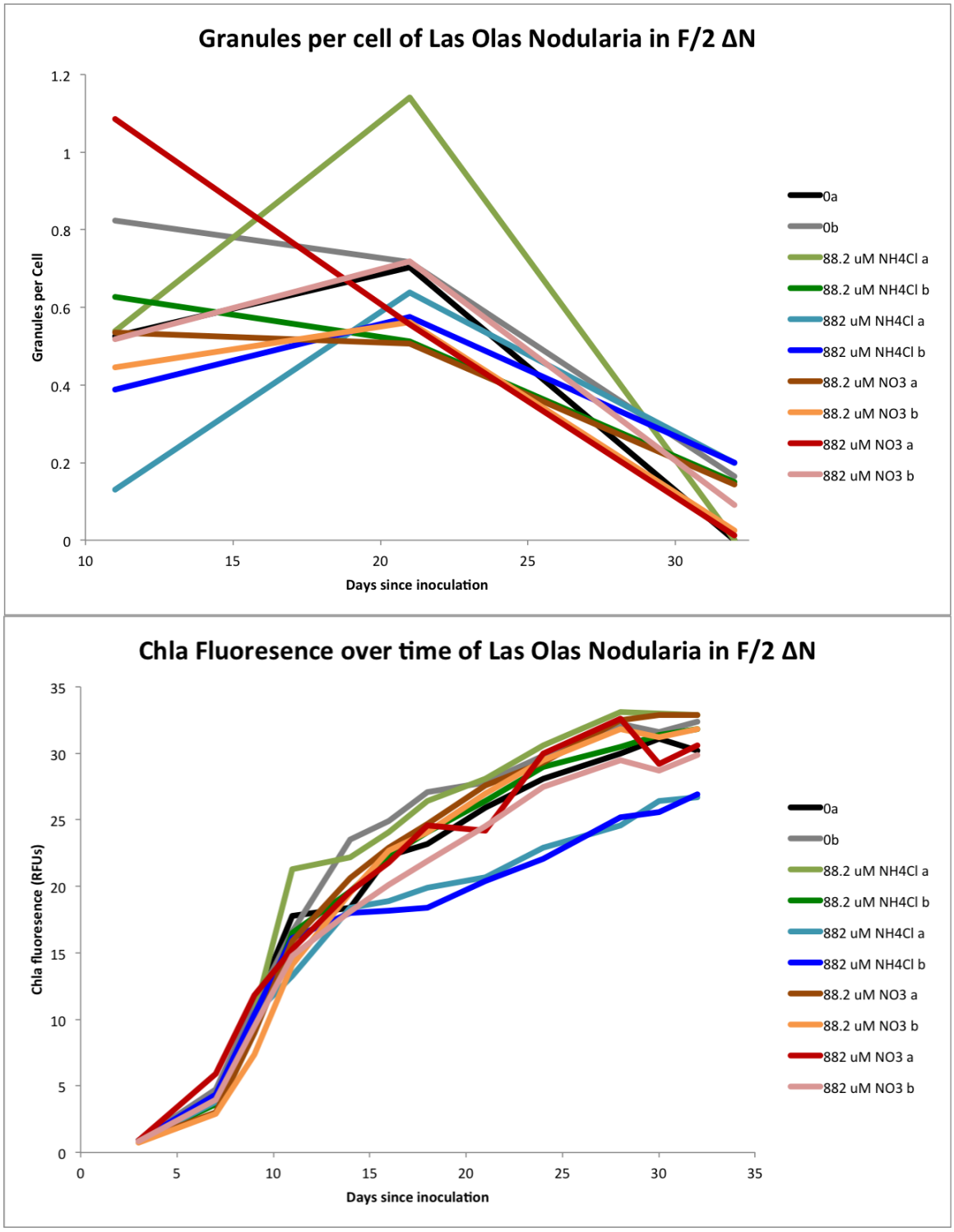

Figure 9: The number of granules per cell of *Nodularia* sp. Las Olas cultures grown in F/2 media made from 100% seawater, under different nitrogen conditions. Two replicates for each treatment are shown.

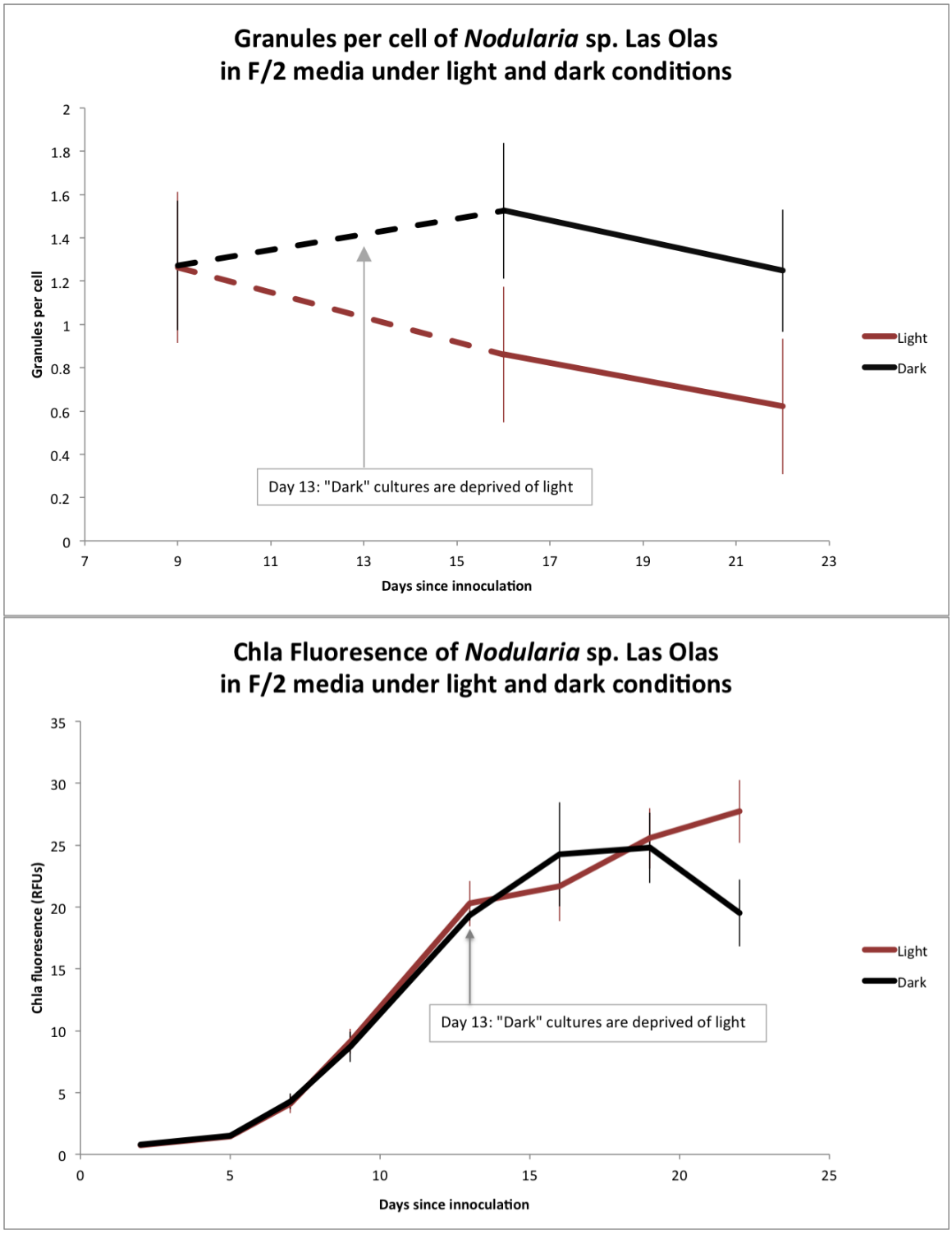

Figure 10: Granules per cell of salt-shocked *Nodularia* sp. Las Olas accompanied by Chla fluorescence of salt-shocked cultures. Data shown are averages from four replicates. Error bars show 95% confidence intervals.

5. FTIR Analysis of *Nodularia* sp. *Las Olas* cell pellets

Staining and non-staining cultures of *Nodularia* sp. *Las Olas* grown in F/2 media at 10%, 50%, and 150% the salinity of seawater, respectively, were also harvested and analyzed via Fourier-transform infrared spectrometry (FTIR) in order to determine whether there were any gross metabolic differences based on the relative abundance of specific chemical bonds present across samples. Of the three samples, the staining *N* sp. *Las Olas* cultures grown at 10% and 50% salinity contained elevated levels of amide and lipid CH_2 and CH_3 bonds compared to cultures grown at 150% salinity (Figure 11).

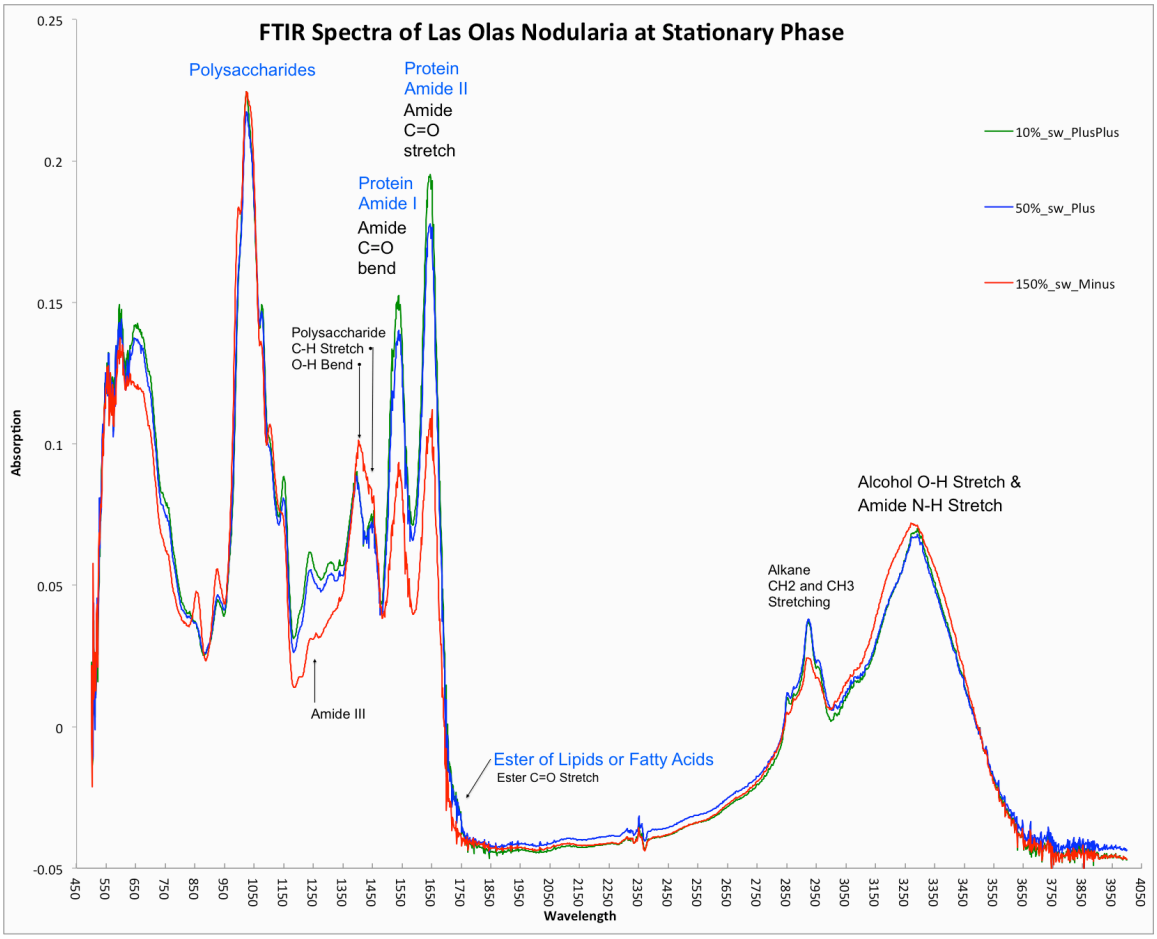

Figure 11: FTIR spectra of staining and non-staining cultures of *Nodularia* sp. Las Olas.

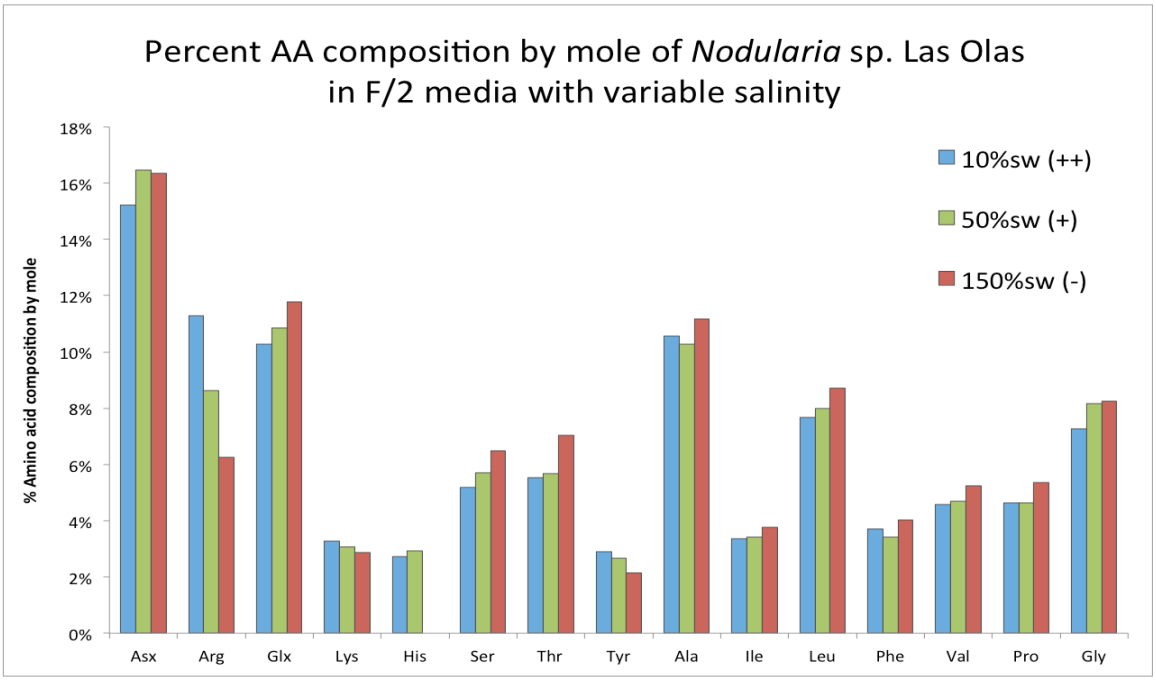

Figure 12: Percent amino acid composition by mole of whole *Nodularia* sp. Las Olas cell pellets grown in 10%, 50%, and 150% seawater. Due to acid hydrolysis, aspartate and asparagine content is listed as "Asx", and glutamate and glutamine content is listed as "Glx".

6. LC-MS Amino Acid Analysis of *Nodularia* sp. *Las Olas* Cell Pellets

These cultures of *Nodularia* sp. *Las Olas* were then hydrolyzed for the purpose of amino acid analysis via liquid chromatography mass spectrometry (LC-MS). The amino acid compositions of the three samples were similar, with the exception of elevated arginine content in the staining, low-salinity cultures. Some small changes were possibly apparent for histidine, lysine, and tyrosine. In particular, the percent composition of arginine appears to be consistent with the patterns of staining shown in Figure 6, with the highest levels of arginine and staining present at the lowest salinities.

In order to better determine whether these differences were due to a CGP-like granule, the CGP granule extraction protocol described by Simon in 1973 was

followed (84), and different fractions from each step were analyzed via HPLC amino acid analysis methods. *Anabaena* sp. PCC 7120, a known CGP producer, was also analyzed as a positive control along with high-staining and low-staining samples of *Nodularia* sp. Las Olas.

Because Nile Red and BODIPY 493/503 stain hydrophobic granules, it was important to determine whether any differences in amino acid composition persisted after lysing the cell pellets using a French pressure cell, and removing water-soluble proteins via repeated washes with water followed by centrifugation.

The amino acid compositions of the water-insoluble pellets showed the same differences in arginine content observed in the whole cell pellets. Aspartate/asparagine content also followed this pattern, with more aspartate/asparagine in the low salinity culture compared to the high salinity culture. Additionally, both cultures of *Nodularia* sp. *Las Olas* had higher arginine and aspartate/asparagine content than *Anabaena* sp. PCC 7120. The removal of water-soluble polypeptides also normalized the previously observed differences in histidine content between the high and low salinity cultures of *Nodularia* sp. *Las Olas*.

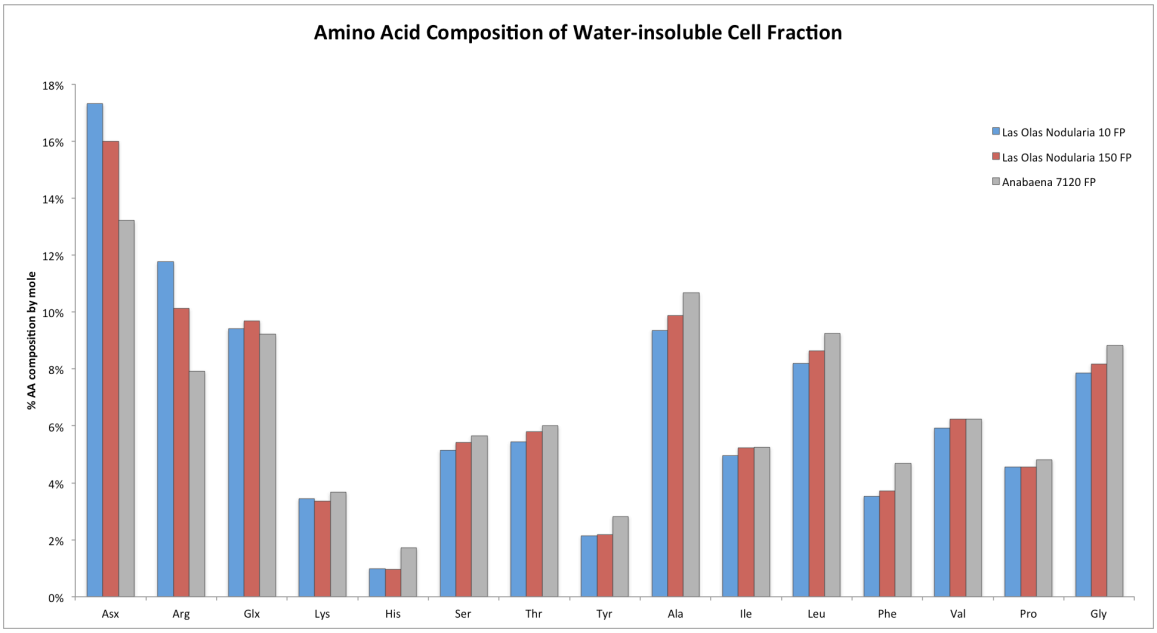

Figure 13: Amino acid composition of water-insoluble cell fraction following French pressure cell treatment and two water washes.

The next CGP purification steps involved a 2% triton-x 100 wash and extraction with 0.1 N HCl, yielding two fractions: a liquid 0.1 N HCl extract which is expected to contain dissolved CGP (66, 84), and a final cell pellet of cellular material insoluble in water, 2% triton-x 100, and 0.1 N HCl. The final cell pellet of insoluble material had an amino acid composition nearly identical to that of the water-insoluble cell fraction, with *Nodularia* sp. *Las Olas* containing more arginine and aspartate/asparagine at lower salinities, and *Anabaena* 7120 containing the lowest percent composition of arginine and aspartate/asparagine.

The liquid CGP-like granule extracts showed an opposite pattern. *Anabaena* sp. PCC 7120 had the highest percent composition of arginine and asparagine/aspartate, and the lowest percent composition of other amino acids.

Extracts from *Nodularia* sp. *Las Olas* grown at high salinity had the second highest percent composition of arginine and aspartate/asparagine, and the second lowest percent composition of other amino acids. HCl extracts from *Nodularia* sp. *Las Olas* grown at low salinity had the lowest percent composition of arginine and aspartate/asparagine, and the highest percent composition of other amino acids.

Thus, the cultures with the highest number of staining granules per cell and highest percent composition of arginine and aspartate/asparagine contained the lowest percent composition of arginine and aspartate/asparagine in their HCl (putative CGP) granule extracts.

This pattern of arginine and aspartate/aspartic acid composition is consistent with BODIPY 493/503 staining of the pellets from each purification step . The staining granules of *Nodularia* sp. *Las Olas* grown at 10% salinity are visible in the cell pellet after lysis via French pressure cell treatment, a 2% Triton-X 100 wash, and extraction with 0.1N HCl (Figure 16). These are the samples in which *Nodularia* sp. *Las Olas* has the highest arginine and aspartate/asparagine content.

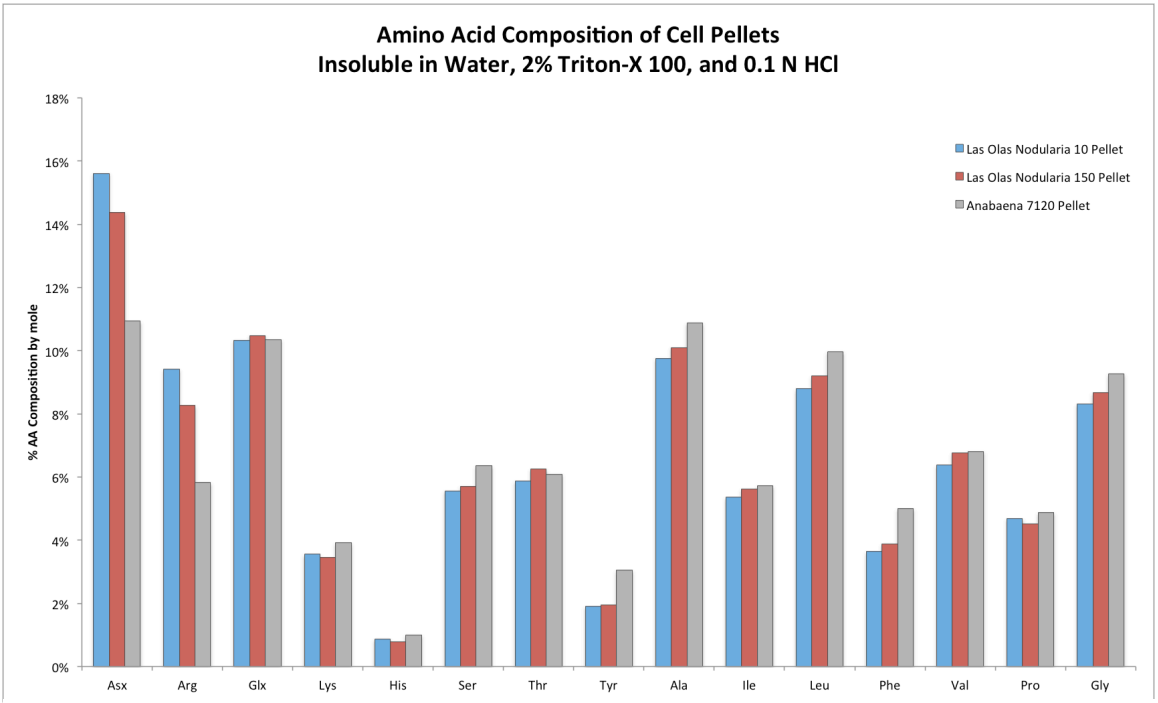

Figure 14: Amino acid composition of final cell pellets insoluble in water, 2% triton-X 100, and 0.1N HCl.

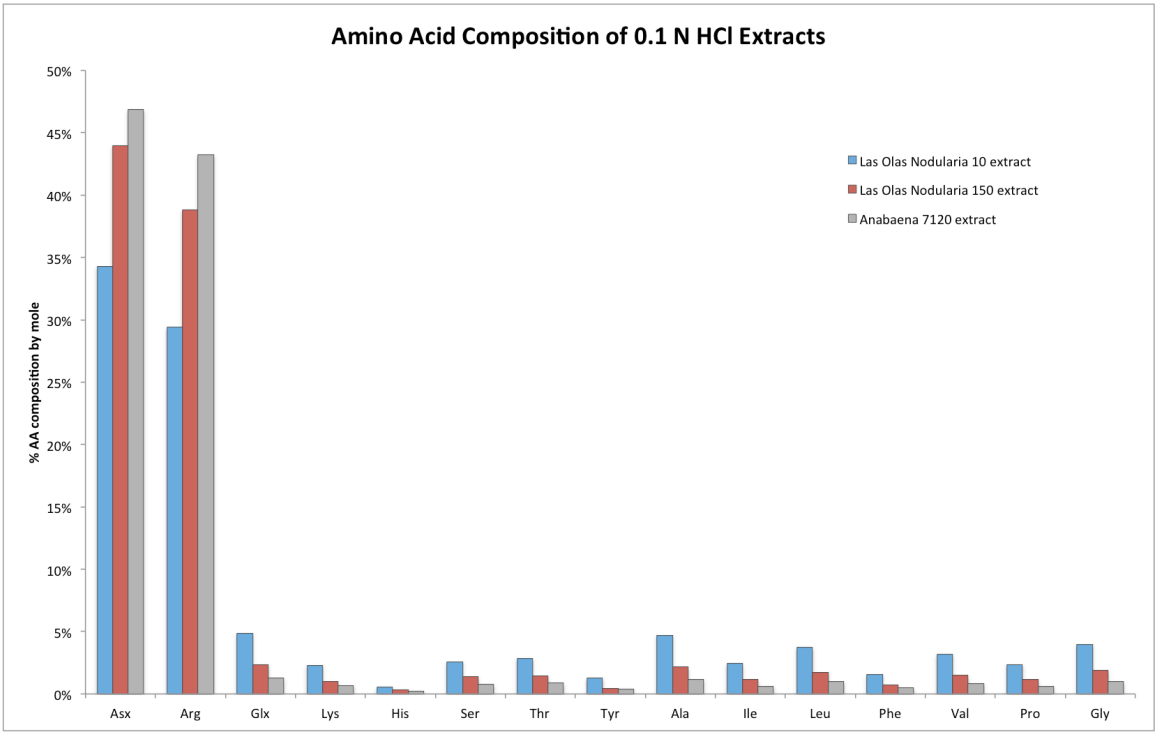

Figure 15: Amino acid composition of 0.1 N HCl extracts containing CGP-like granules.

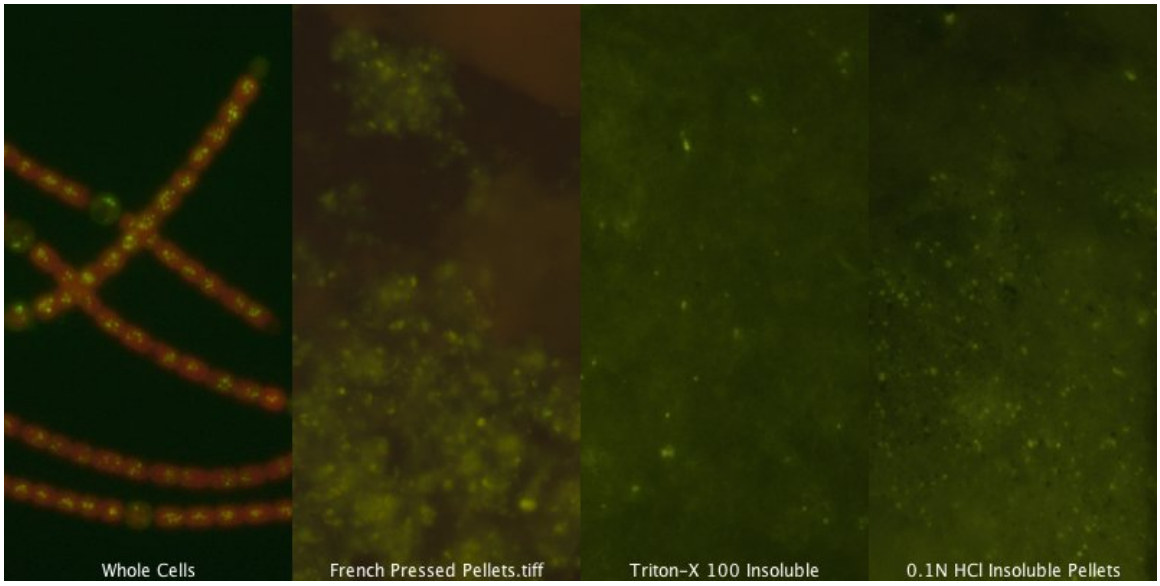

Figure 16: BODIPY 493/503 staining of cell pellets subject to amino acid analysis.

7. GC-MS and TLC analyses of *Nodularia* sp. *Las Olas* and *Phormidium* cf. *irriguum* CCALA 759 Lipid Extracts

The two staining granule accumulators which did not produce PHAs, *Nodularia* sp. *Las Olas* and *Phormidium* cf. *iriguum* CCALA 759, were analyzed for lipid content using thin layer chromatography (TLC) and gas chromatography-mass spectrometry (GC-MS), along with the non-staining strains *Nodularia* sp. *WHNOD* and *Phormidium autumnale* UTEX 1580.

The lipid profiles of *Nodularia* sp. *WHNOD* and *Nodularia* sp. *Las Olas* grown at 10% salinity and 150% salinity did not show any notable differences in quantity or composition of lipids accumulated. Despite some variation, the magnitude of variation was less than the variation observed in the C19 methyl ester standard, which averaged an integrated peak area of 20.256 +/- 0.00541 ($\bar{x}$ +/- 95% CI) units

of abundance, based on relative intensity. The ranges of abundance for each lipid group were well within this margin of error (Figure 17). Furthermore, the lack of variability between the lipid profiles of *Nodularia* sp. *Las Olas* grown at 10% and 150% salinity was consistent between an additional pair of biological replicates, which had been extracted with twice the volume of hexane.

By contrast, there were a few notable differences between the lipid extracts of *Phormidium* cf. *Irriguum* CCALA 759 and *Phormidium autumnale* UTEX 1580. Although the non-staining strain, *P. autumnale* UTEX 1580 produced more 9-hexadecanoic acid methyl esters (34.7% probability NIST match) than *P.* cf. *irriguum* CCALA 759, the staining strain *P.* cf. *iriguum* CCALA 759 produced lipids that appear to be 7,10 hexadecanoic acid methyl esters (46.0% probability NIST match) and 8-heptadecene (two peaks, 15.8% and 18.6% probability NIST match), neither of which were found in *P. autumnale* UTEX 1580.

Raw lipid extracts were also analyzed via thin layer chromatography, in order to determine whether there are differences between the lipids of each strain that are not apparent after esterification. Both the staining and non-staining strains of *Phormidium* and *Nodularia* shared one spot in the neutral lipid portion of the TLC plate (Figure 19), and GC-MS analysis of this spot showed no differences in lipid composition (Figure 20). The spots were comprised of lipid groups consistent with the hexadecanoic and octadecanoic acid peaks observed during analysis of vegetable oil controls (84.7% and 75.8% probability NIST match, respectively) and complete lipid profiles (Figures 17 and 18). A third peak which was not observable during

analysis of complete lipid profiles was also found. It which tentatively appears to be tetradecane, 2,6,10 trimethyl, based on a 9.21% probability NIST match for the *Nodularia* spectra, and an 11.2% match for the *Phormidium* spectra (Figure 19).

A second neutral lipid spot was observed only in *Nodularia* sp. *Las Olas* grown at 10% salinity, and the location of this spot was similar to the vegetable oil control (Figure 19). GC-MS analysis reveals that these neutral lipids are comprised of hexadecanoic and octadecanoic acids (Figure 21).

Additionally, there were two polar lipid spots present in *Nodularia* sp. *WHNOD* and *Nodularia* sp. *Las Olas* grown at 10% salinity, but not in *N.* sp. Las Olas grown at 150% salinity. These spots were also found to be comprised of hexadecanoic and octadecanoic acids (Figures 22 and 23).

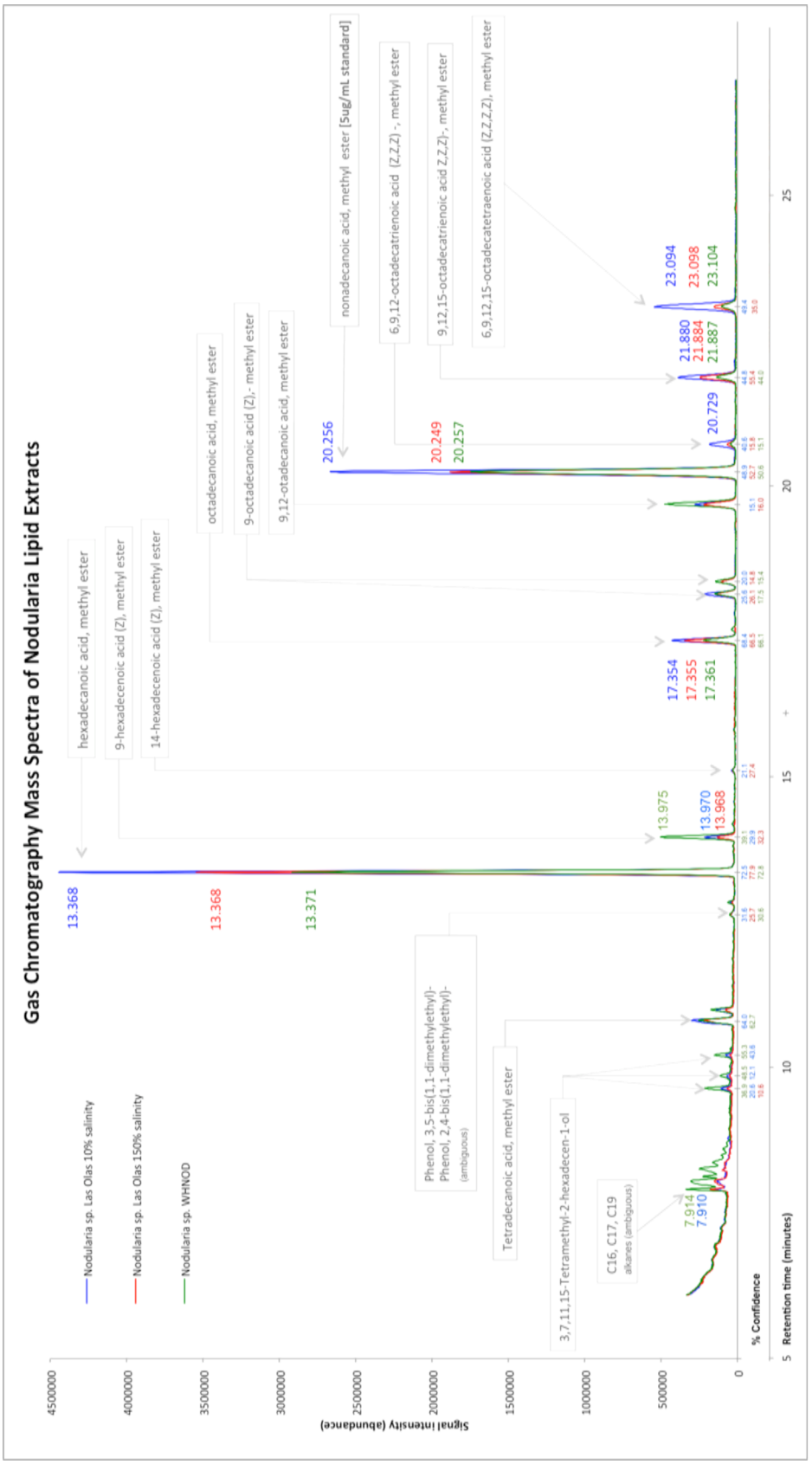

Figure 17: GC-MS spectra of lipid extracts from *Nodularia* sp. WHNOD and *Nodularia* sp. Las Olas grown at 10% and 150% salinity. Integrated areas of significant peaks are color-coded, beside each peak. Peak labels are based on NIST library searches, and are consistent across all samples, including a vegetable oil control. Percent confidence for NIST matches are given below each peak.

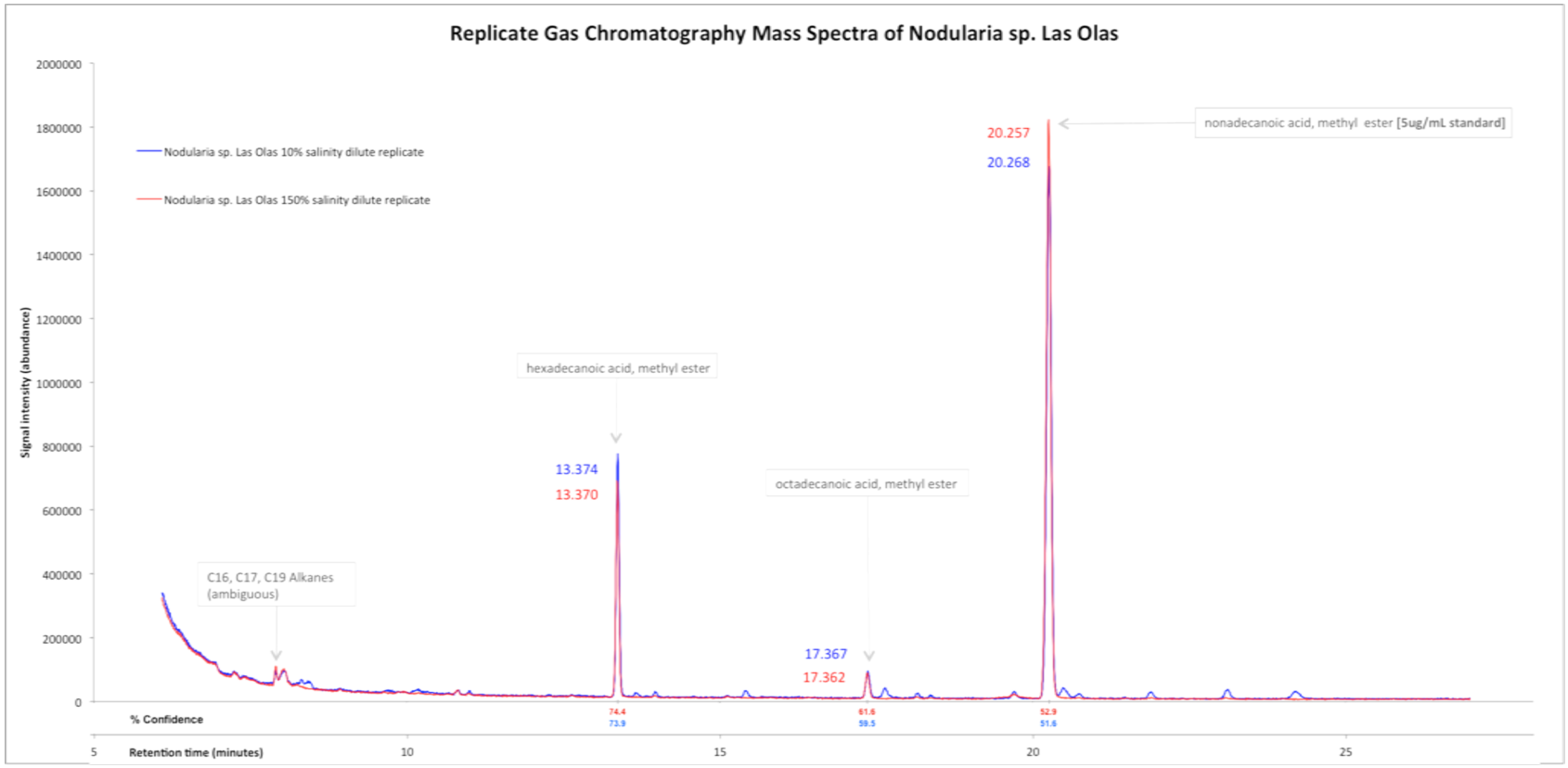

Figure 18: GC-MS spectra of a second, more dilute pair of lipid extracts from *Nodularia* sp. Las Olas cultures grown at 10% and 150% salinity, extracted with 500ul instead of 330 µl hexanes. Integrated areas of significant peaks are color-coded beside each peak. Peak labels are based on NIST library searches, and are consistent across all samples, including a vegetable oil control. Percent confidence for NIST matches are given below each peak.

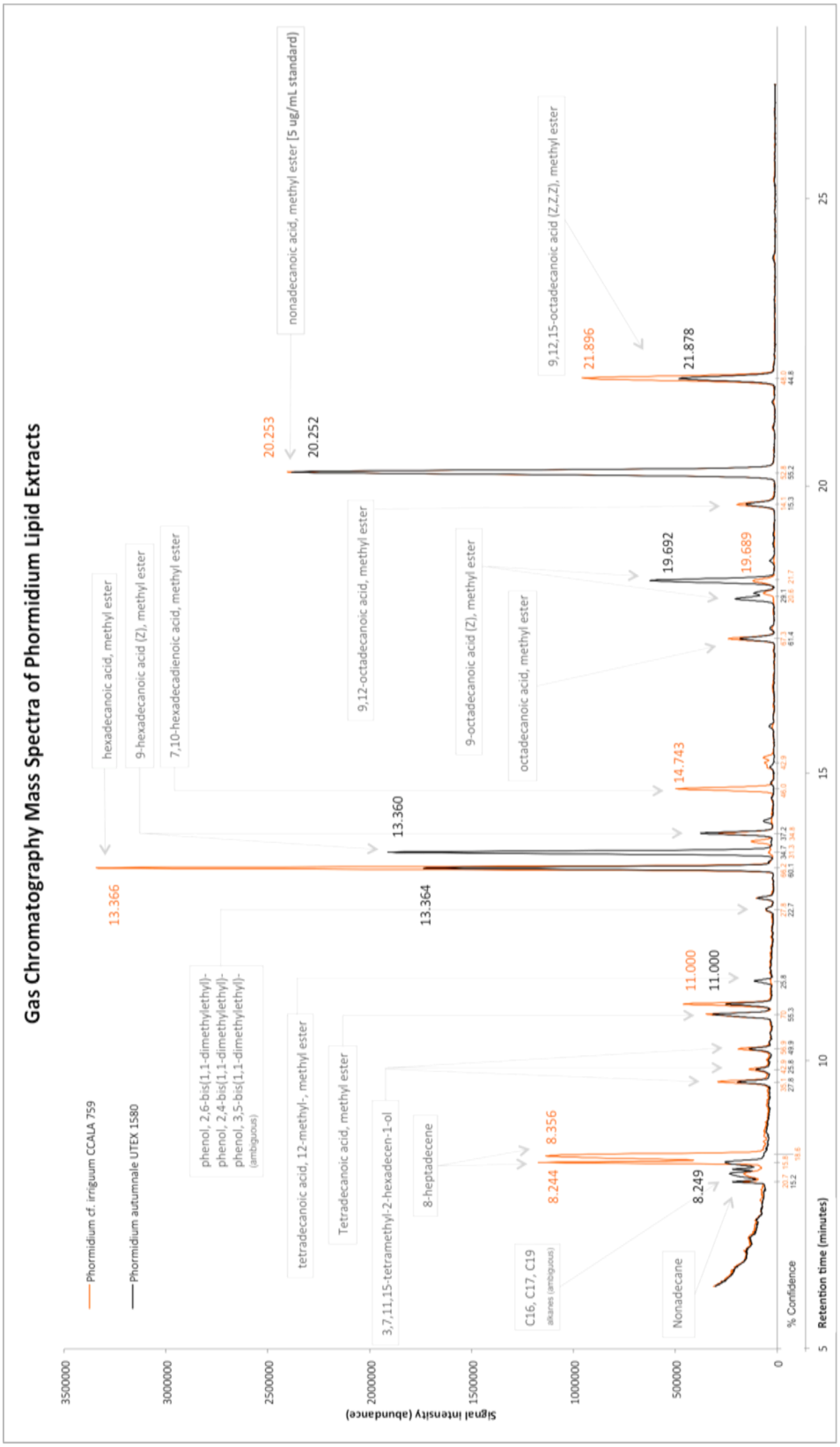

Figure 19: GC-MS spectra of lipid extracts from *Phormidium* cf. irriguum CCALA 759 and *Phormidium* autumnale UTEX 1580. Integrated areas of significant peaks are color-coded beside each peak. Peak labels are based on NIST library searches, and are consistent across all samples, including a vegetable oil control. Percent confidence for NIST matches are given below each peak.

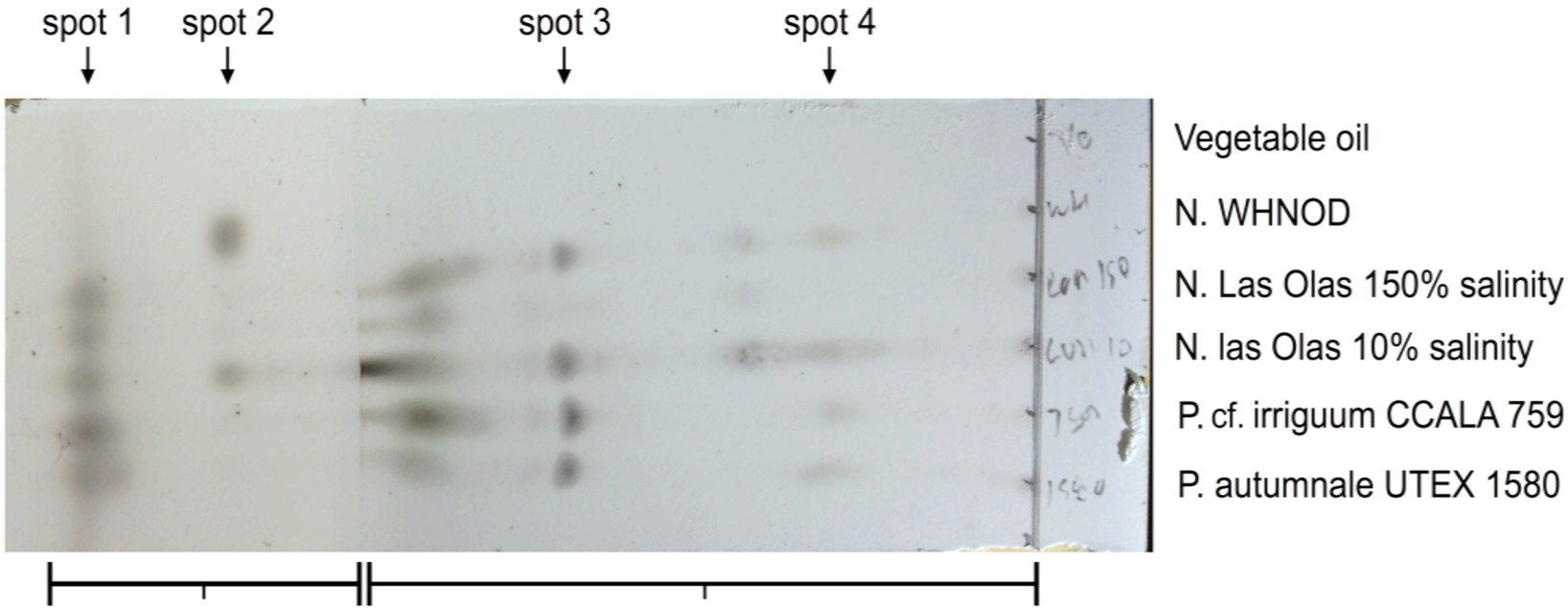

Figure 20: TLC plates of *Nodularia* sp. Las Olas at 10% and 150% salinity, UTEX 1580, CCALA 759, *Nodularia* sp. WHNOD, and vegetable oil using a two- solvent system.

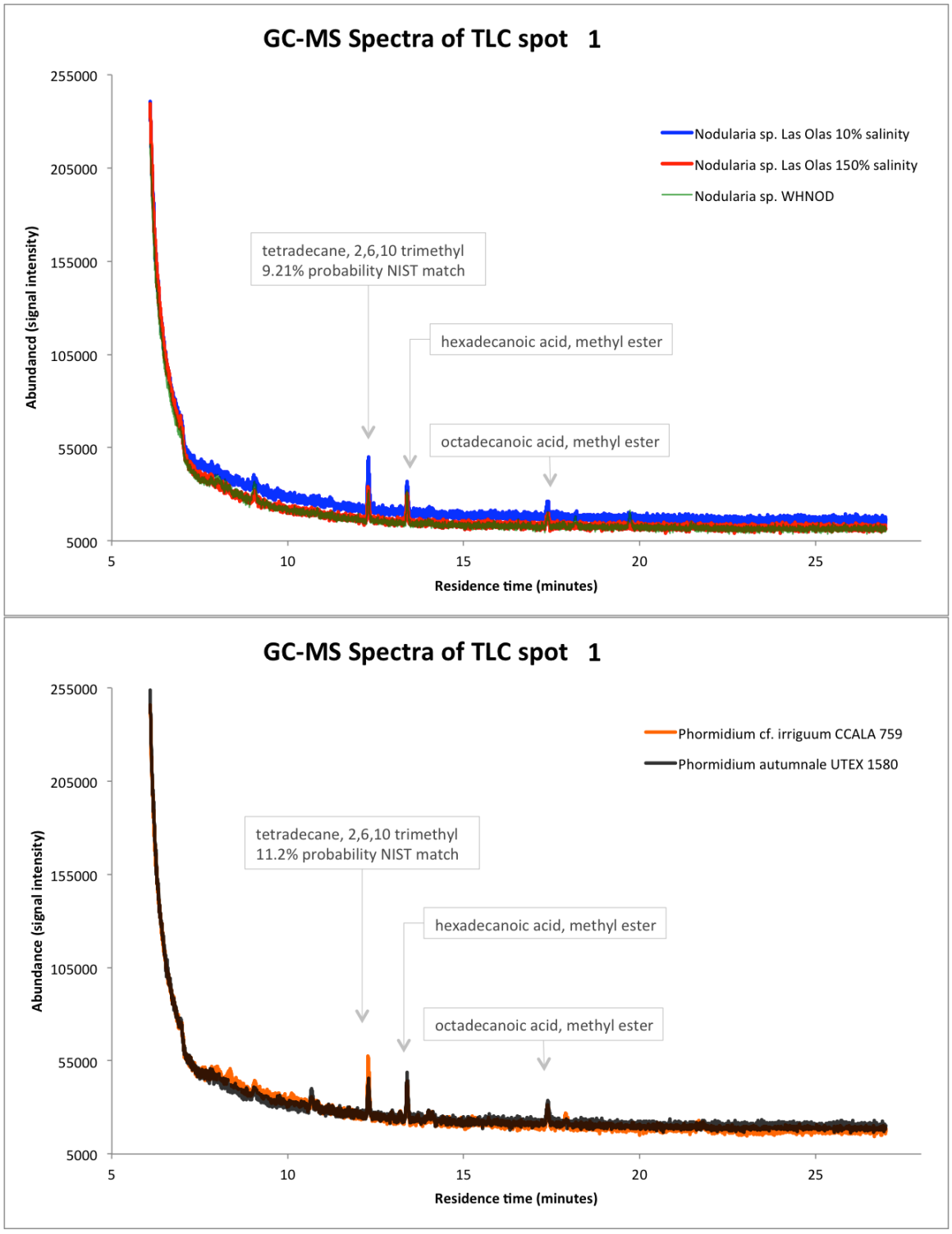

Figure 21: GC-MS spectra of TLC spot 1 (as labeled in Figure 20).

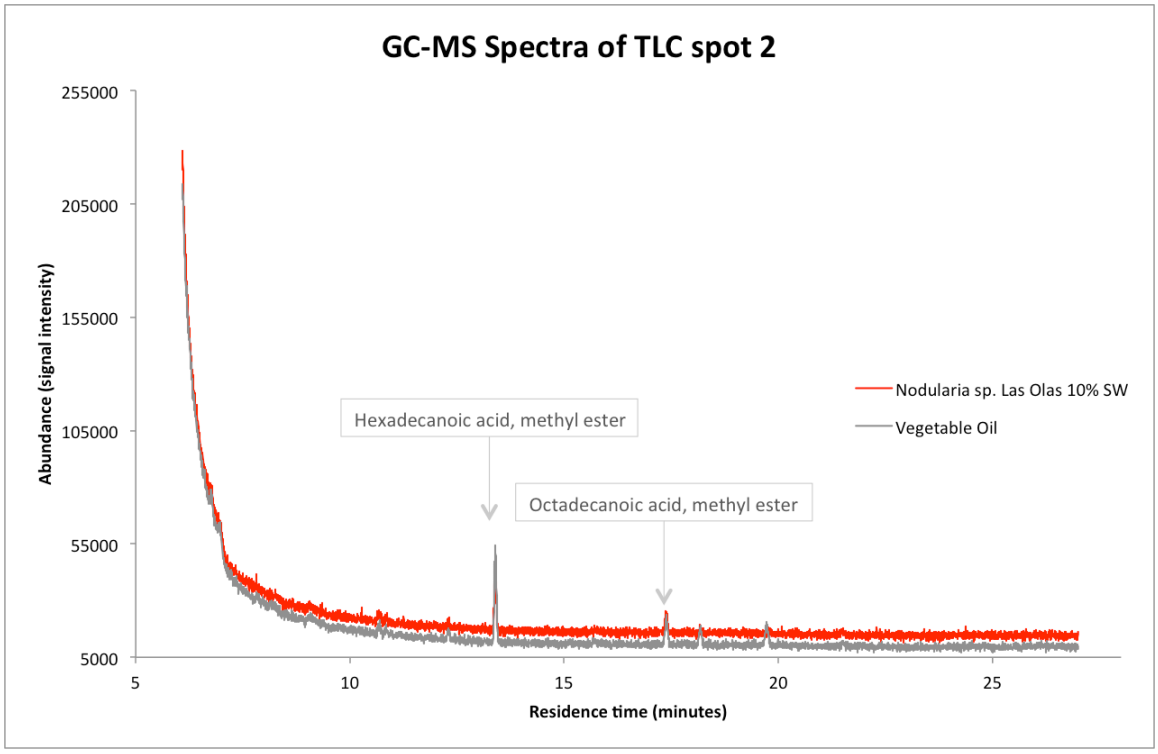

Figure 22: GC-MS spectra of TLC spot 2 (as labeled in Figure 20).

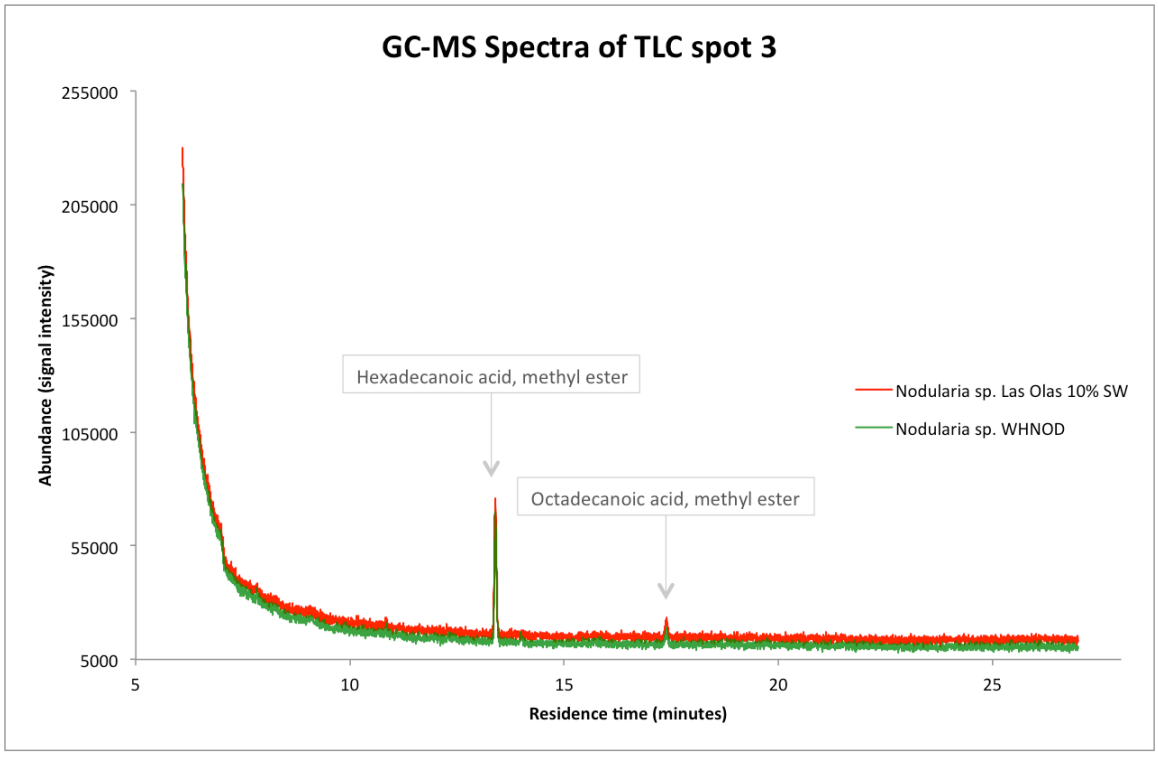

Figure 23: GC-MS spectra of TLC spot 3 (as labeled in Figure 20).

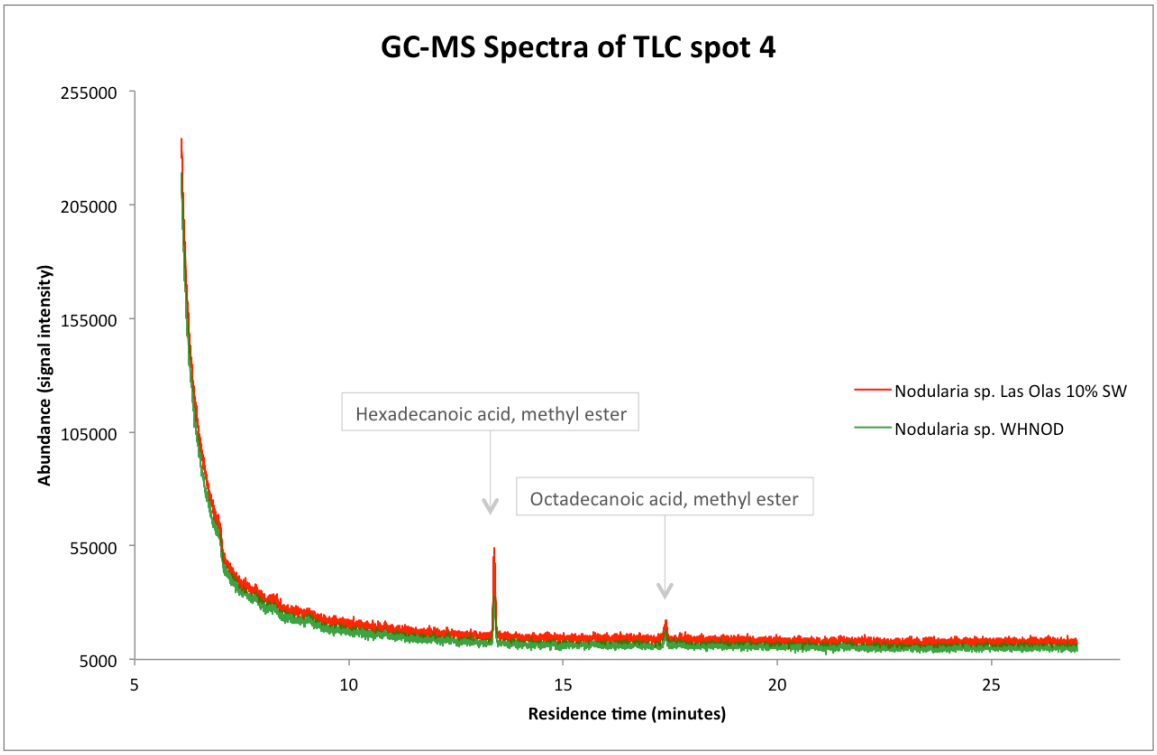

Figure 24: GC-MS spectra of TLC spot 3 (as labeled in Figure 20).

Results are currently being prepared for submission for publication of the material. Hong, Karl; Palenik, Brian. The thesis author was the primary author of this material, under the guidance of the principal investigator, Brian Palenik.

Discussion

1. Characterization of Polyhydroxyalkanoates

One goal of this study was to characterize the evolutionary history of polyhydroxyalkanoate biosynthesis within the phylum Cyanobacteria.

PHA synthase *PhaC* and Nile Red/BODIPY staining was found in the three halotolerant and freshwater strains of *Synechocystis* spp. *WHSYN*, *LSNM*, and *CGF*-1 characterized in this study. Additionally, the presence of PHB was confirmed via proton NMR in *Synechocystis* sp. *WHSYN*. The model strain *Synechocystis* sp. PCC 6803 was also screened via staining and PCR to verify the methods used in this study. The widespread occurrence BODIPY 493/503-staining and PHA synthase subunit PhaC in both halotolerant and freshwater strains of *Synechocystis* suggests that PHA biosynthesis is highly conserved within the genus. This makes *Synechocystis* an even stronger candidate for further bioprospecting and the development of PHA bioplastics.

Additionally, PHA accumulation was also found in the novel *Phormidium-like* sp. CGFILA. Although some PHA accumulation has previously been observed in the genus *Phormidium*, this study is the first genetic characterization of a *Phormidium* PHA biosynthesis gene. This occurrence and genetic characterization of *Phormidium* PHA biosynthesis is especially useful because the genus *Phormidium* is polyphyletic (86), leading to confusion as to which *Phormidium* produce PHAs, and which do not. Furthermore, even within the monophyletic sub-clade of *Phormidium* where PHA biosynthesis is found, most strains of *Phormidium* do not produce polyhydroxyalkanoates based on staining, phaC PCR screening, and in some

instances, ^{1}H NMR (Table 3). It is unclear as to what evolutionary conditions drove the loss of PHA accumulation in some *Phormidium* but not others; however, it is clear that PHA biosynthesis is found in a subset of organisms belonging to the clade of *Phormidium* in which da Silva Malone, et al. proposed reclassification as *Cephalothrix* in 2015 (86).

The characterization of this novel *Phormidium* phaC gene also gives evidence for horizontal gene transfer (HGT) within the phylum Cyanobacteria. Although no instances of horizontal gene transfer between cyanobacteria and eubacteria were found, three instances of potential HGT within the phylum Cyanobactaria were observed (Figures 4 and 5). Of these three instances, only the case of HGT between recent ancestors of *Pleurocapsa* sp. PCC 7327 and the novel *Phormidium*-like sp. CGFILA is supported by at least moderate bootstrap values, 94 and 68 for 16s/23s rRNA and phaC/phaE, respectively (Figure 4). The HGT event proposed by Jane modeling between ancestors of the genera *Synechocystis* and *Arthrospira* had some bootstrap support; however, a bootstrap value of 45 at the relevant node of the phaC/phaE trees (Figures 4c) is not high enough to propose any meaningful differences between the 16s/23s and phaC/phaE phylogenies, especially between genera as closely related as *Synechocystis* and *Arthrospira*. HGT between recent ancestors of *Microcoleus* Vaginatus FGP-2 and *Gloeocapsa* sp. PCC 7428 is currently unsupported due to the rooting of the tree.

Thus, a novel *phormidium* phaC genewas characterized, lending insight as to which *Phormidium* produce polyhydroxyalkanoates. Additionally, one moderately-supported instance of HGT of a PHA synthase gene within the phylum Cyanobacteria

was found, involving recent ancestors of *Pleurocapsa* sp. PCC 7327 and the novel *Phormidium*-like sp. *CGFILA.* Further work involving the other two PHA biosynthesis genes, phaA and phaB would be useful to further explore this story, as well as to better determine whether the other two apparent incongruences represent additional cases of HGT.

2. Characterization of Granules in *Nodularia* sp. *Las Olas*

Furthermore, two BODIPY-staining, non-PHA granules were found in the cyanobacteria *Nodularia* sp. *Las Ola*s and *Phormidium* cf. *irriguum* CCALA 759. These two strains belong to clades of cyanobacteria associated with widespread phaC gene loss (Figure 3), and they do not appear to produce polyhydroxyalknanoates based on phaC PCR screening and ^{1}H NMR (Table 3 and Figure 2).

Granule accumulation by *Nodularia* sp. *Las Olas* is induced during stationary phase at low salinity (Figures 6a, 6b, and 7), and phosphate limitation (Figure 8). Furthermore, placing cultures in darkness also seems to have a small positive effect on granule accumulation (Figure 10). High accumulation during stationary-phase, nutrient-limited conditions is consistent with the accumulation of many cyanobacterial carbon/nutrient storage compounds, such as polyhydroxyalkanoates, cyanophycin granule polypeptides, and lipid droplets (12, 27, 60). However, granule accumulation does not appear to be affected by nitrogen status or nitrogen source (Figure 9), whereas known PHA, CGP, and LD granules of filamentous, nitrogen-fixing cyanobacteria all tend to be strongly influenced by nitrogen status and/or nitrogen source (12, 27, 60).

FTIR analysis of whole cell pellets of *N.* sp. *Las Olas* reveals that staining cultures contain more amide and lipid bonds than non-staining cultures (Figure 11). In particular, the pattern of abundance of amide bonds closely resembles the patterns of staining observed in Figures 6a and 6b. Cultures of *N.* sp. *Las Olas* grown at 10% salinity had more granules per cell and more amide bonds than cultures grown at 50% salinity, and cultures grown at 50% salinity had more granules per cell and amide bonds than cultures grown at 150% salinity (Figures 6a,6b, and 11). In contrast, cultures of *N.* sp. *Las Olas* grown at 10% salinity had more granules per cell but roughly the same amount of lipid bonds as cultures grown at 50% salinity, even though both 10% and 50% salinity cultures had more lipid bonds than those grown at 150% salinity. Thus, although lipid content may be a component of the staining granules produced by *N.* sp. *Las Olas,* these granules more significantly appear to be comprised of amide bonds.

GC-MS and TLC analysis of lipid profiles from biological replicates of *N.* sp. *Las Olas,* grown at 10% and 150% seawater lend further insight into the role lipids may play in these granules. Although GC-MS analyses of esterified lipid extracts from *N.* sp. *Las Olas* and the non-staining *N.* sp. *WHNOD* showed little difference in composition or quanitity of alkanes, long-chain alcohols, and fatty acids produced (Figure 17), TLC analysis of lipid extracts prior to esterification reveals that the lipids produced by *N.* sp. *Las Olas* at 10% salinity are indeed different from those produced at 150% salinity, and those produced by *N.* sp. *WHNOD* (Figure 20). In particular, *N.* sp. *Las Olas* at 10% salinity appears to be accumulating neutral lipids similar to vegetable oil triacylglycerols, as well as a few polar lipids that are not

present in high abundance at 150% salinity. The lipids present in the TLC spots that were found in *N.* sp. *Las Olas* at 10% salinity but not at 150% were once again found to be no different from the lipids present in the lipid extracts of of *N.* sp. *Las Olas* grown at 150% salinity, and of *N.* sp. *WHNOD* (Figures 22, 23, and 24). Thus, despite similarities in overall composition and quantity of lipid groups between high and low salinity cultures of of *N.* sp. *Las Olas*, it appears that many these lipids are modified in ways that are obfuscated by methanol esterification. This is consistent with the FTIR data which suggests that lipids may be a secondary component, but do not appear to be a primary component of the BODIPY 493/503-staining granules of of *N.* sp. *Las Olas.*

HPLC amino acid analysis further supports the hypothesis that amino acids are a primary component of these granules. Amino acid analysis of whole cell pellets reveal that the percent composition of arginine increases as salinity decreases, in a manner consistent both BOIDPY 493/503 staining and the relative quantities of amide bonds observed via FTIR (Figures 6b, 11, and 12). After removing water-soluble proteins, which are not stained by BODIPY 493/503, a very cyanophycin-like pattern emerges. Lysed and water-washed cell pellets of *N.* sp. *Las Olas* grown at 10% salinity have a higher percent composition of arginine and aspartate/asparagine than cultures grown at 150% salinity, while all other amino acid levels are roughly equivalent (Figure 13). This pattern persists after washing the pellets with 2% triton-X 100, behaving in a manner consistent with the amino acid composition of cell pellets from *Anabaena* sp. PCC 7120, a known producer of cyanophycin granules that are not stained by BODIPY 493/503 (Figure 14). Unlike

the CGP-containing cell pellets of *Anabaena* sp. PCC 7120, however, much of the arginine and aspartate/asparagine in *Nodularia* sp. *Las Olas* remained in the cell pellet after extraction with 0.1N HCl, instead of being solubilized by the 0.1N HCl (Figures 14, 15 and 16).

Prior to extraction with 0.1N HCl, *N.* sp. *Las Olas* grown at 10% salinity contained the highest percent composition of arginine and aspartate, followed by *N.* sp. *Las Olas* grown at 150% salinity, and finally *Anabaena* sp. PCC 7120 (Figures 13 and 14). This pattern was consistent in the cell pellets following extraction with 0.1N HCl (Figure 15). However, the CGP-containing 0.1 N HCl extracts followed an opposite pattern, with *Anabaena* sp. PCC 7120 extracts containing the highest percentage of arginine and aspartate/asparagine, followed by *N.* sp. *Las Olas* grown at 150% salinity, and *N.* sp. *Las Olas* grown at 10% salinity.

Thus, *N.* sp. *Las Olas* is producing elevated levels of a cyanophycin-like compound rich in arginine and aspartate/asparagine at low salinity, and this compound is less soluble than cyanophycin in 0.1N HCl. Furthermore, this cyanohycin-like compound is negatively correlated with the amount of typical cyanophycin present in 0.1 N HCl extracts, suggesting that arginine and aspartate/asparagine are preferentially being incorporated into some other cyanophycin-like compound, rather than CGP granules, as currently understood.

Because *Nodularia* sp. Las Olas was isolated in an estuary, and the number of granules per cell is strongly associated with decreasing salinity, a reasonable explanation would be that these granules help *Nodularia* sp. Las Olas cope with hyposmotic conditions, sequestering water-soluble arginine and/or aspartate

osmolites for later use in a water-insoluble form that is independent from nitrogen-mediated regulation of CGP synthesis and degradation. Indeed, many species of *Nodularia* have been found brackish water environments with special adaptations for thriving across wide ranges of salinity (7, 87, 88). However, this explanation does not quite explain why a dye like BODIPY 493/503, which fluoresces only in hydrophobic environments, would stain polyarginine and/or polyaspartate compounds unless they are somehow bound to neutral lipids or associated with ions or molecules that balance the charges of the amino acid residues.

An related explanation would be that these granules are instead a more general carbon and/or nutrient storage response to physiological stress conditions, and the accumulation of this CGP-like granule could be unresponsive to changing nitrogen conditions because the nitrogen-fixing *N.* sp. *Las Olas* is simply not stressed by nitrate-limitation. This is supported by Figure 8, which shows that the number of granules accumulated by *N.* sp. *Las Olas* increases under phosphate limitation.

Further work must be done in order to determine whether levels of this CGP-like granule are also correlated with the increased staining observed at low phosphate levels, relative to high phosphate levels (Figure 8). This would involve repeating the FTIR and HPLC amino acid experiments performed with *N.* sp. *Las Olas* grown at high and low salinity. If these staining granules are rich in arginine and aspartate/asparagine, then the amino acid compositions of phosphate-limited *N.* sp. *Las Olas* cultures should be similar to those of *N.* sp. *Las Olas* at low salinity.

Possible links between this CGP-like compound and the differences in lipids found via TLC (Figure 20) can be explored by determining the amino acid

composition of the pellets and extracts resulting from the isopropanol/hexane lipid extraction protocol. The granules produced by *N.* sp. *Las Olas* must be hydrophobic in order to exhibit BODIPY 493/503 fluorescence. If the CGP-like particle is hydrophobic then I would expect to find arginine and aspartate in the hexane extracts of staining *N.* sp. *Las Olas* Cultures, but not in the hexane extracts of non-staining cultures.

Nevethertheless, it has been demonstated that *Nodularia* sp. *Las Olas* does accumulate a novel BODIPY 493/503-staining granule that appears to contain poly-arginine and poly-aspartate/asparagine amino acid residues, with solubility characteristics different from those of cyanophycin granule polypeptides, as currently understood.

3. Characterization of Granules in *Phormidium* cf. *irriguum* CCALA 759

The staining granules of stationary phase *Phormidium* cf. *irriguum* CCALA 769 were small, numerous, and not localized in the center of cells, unlike the granules produced by *Phormidium*-like sp. *CGFILA*, *Nodularia* sp. *Las Olas* (Figure 1), and *Nostoc punctiforme* during stationary phase (12). They appear similar to the small, delocalized lipid droplets produced by *N. punctiforme* during exponential phase, which contained a higher proportion of alkanes compared to the larger, more centralized stationary phase droplets (54).

This observation is supported by the GC-MS analysis of lipid extracts. With respect to fatty acid accumulation, the GC-MS lipid profile of *P.* cf. *irriguum* CCALA 759 differed from that of the non-staining *Phormidium* autumnale UTEX 1580 in

composition, but not necessarily quantity. While both strains produced many C16 and C18 fatty acids, *P. autumnale* UTEX 1580 produced elevated levels of 9-hexadecenoic acids, whereas *P.* cf. *irriguum* CCALA 759 produced 7,10 hexadecenoic acids (46% probability NIST match) not found in the other *Phormidium* or *Nodularia* strains (Figure 19).

P. cf. *irriguum* CCALA 759 extracts were found to contain elevated levels of alkanes, relative to the other strains in this study. These alkanes appear to be 8-heptadecene (two peaks, 15.8% and 18.6% probability NIST matches) and signals of similar magnitude with the same residence time were not found in *P. autumnale* UTEX 1580 (Figure 19), or any of the *Nodularia* strains analyzed in this study.

GC-MS analysis of TLC scrapings showed that the neutral lipids of *P.* cf. *irriguum* CCALA 759 contain hexadecanoic acids, octadecanoic acids, and an unidentified alkane which tentatively appears to be tetradecane, 2,6,10 trimethyl (11.2% probability NIST match). Signal in the GC-MS spectra for the TLC scrapings was not high enough to convincingly identify this alkane, nor quantify relative quantities of alknaes (Figure 21).

Further work regarding granule induction, as well as optimization of the TLC GC-MS protocol with alkane standards must be done in order to determine the exact composition of the small, de-localized granules produced by *P.* cf. *irriguum* CCALA 759, which appear to contain elevated levels of alkanes.

In summary, the Nile Red and BODIPY 493/503-staining granules from three different classes of cyanobacterial carbon storage compounds were characterized in six cyanobacteria. The characterization of these compounds presents exciting

opportunities and insights for the development of cyanobacteria bioproducts made from lipids, polyamides, and polyhydroxyalkanoates.

References

1. US EPA O. Inventory of U.S. Greenhouse Gas Emissions and Sinks. Reports and Assessments.

2. Jambeck JR, Geyer R, Wilcox C, Siegler TR, Perryman M, Andrady A, Narayan R, Law KL. 2015. Plastic waste inputs from land into the ocean. Science 347:768–771.

3. Andrady AL. 2011. Microplastics in the marine environment. Mar Pollut Bull 62:1596–1605.

4. Thompson RC, Moore CJ, vom Saal FS, Swan SH. 2009. Plastics, the environment and human health: current consensus and future trends. Philos Trans R Soc B Biol Sci 364:2153–2166.

5. Singh B, Sharma N. 2008. Mechanistic implications of plastic degradation. Polym Degrad Stab 93:561–584.

6. Ducat DC, Way JC, Silver PA. 2011. Engineering cyanobacteria to generate high-value products. Trends Biotechnol 29:95–103.

7. Bolch CJS, Orr PT, Jones GJ, Blackburn SI. 1999. Genetic, Morphological, and Toxicological Variation Among Globally Distributed Strains of Nodularia (Cyanobacteria). J Phycol 35:339–355.

8. Welker M, Maršálek B, Šejnohová L, von Döhren H. 2006. Detection and identification of oligopeptides in Microcystis (cyanobacteria) colonies: Toward an understanding of metabolic diversity. Peptides 27:2090–2103.

9. Beck C, Knoop H, Axmann IM, Steuer R. 2012. The diversity of cyanobacterial metabolism: genome analysis of multiple phototrophic microorganisms. BMC Genomics 13:56.

10. Singh JS, Kumar A, Rai AN, Singh DP. 2016. Cyanobacteria: A Precious Bio-resource in Agriculture, Ecosystem, and Environmental Sustainability. Front Microbiol 7.

11. Asada Y, Miyake M, Miyake J, Kurane R, Tokiwa Y. 1999. Photosynthetic accumulation of poly-(hydroxybutyrate) by cyanobacteria--the metabolism and potential for CO2 recycling. Int J Biol Macromol 25:37–42.

12. Peramuna A, Summers ML. 2014. Composition and occurrence of lipid droplets in the cyanobacterium Nostoc punctiforme. Arch Microbiol 196:881–890.

13. Kacmar J, Carlson R, Balogh SJ, Srienc F. 2006. Staining and quantification of poly-3-hydroxybutyrate in Saccharomyces cerevisiae and Cupriavidus necator cell populations using automated flow cytometry. Cytom Part J Int Soc Anal Cytol 69:27–35.

14. Rumin J, Bonnefond H, Saint-Jean B, Rouxel C, Sciandra A, Bernard O, Cadoret J-P, Bougaran G. 2015. The use of fluorescent Nile red and BODIPY for lipid measurement in microalgae. Biotechnol Biofuels 8:42.

15. Anderson AJ, Dawes EA. 1990. Occurrence, metabolism, metabolic role, and industrial uses of bacterial polyhydroxyalkanoates. Microbiol Rev 54:450–472.

16. Chuah J-A, Tomizawa S, Yamada M, Tsuge T, Doi Y, Sudesh K, Numata K. 2013. Characterization of Site-Specific Mutations in a Short-Chain-Length/Medium-Chain-Length Polyhydroxyalkanoate Synthase: In Vivo and In Vitro Studies of Enzymatic Activity and Substrate Specificity. Appl Environ Microbiol 79:3813.

17. Knoll M, Hamm TM, Wagner F, Martinez V, Pleiss J. 2009. The PHA Depolymerase Engineering Database: A systematic analysis tool for the diverse family of polyhydroxyalkanoate (PHA) depolymerases. BMC Bioinformatics 10:89.

18. Sudesh K, Abe H, Doi Y. 2000. Synthesis, structure and properties of polyhydroxyalkanoates: biological polyesters. Prog Polym Sci 25:1503–1555.

19. Koning G de. 1995. Physical properties of bacterial poly((*R*)-3-hydroxyalkanoates). Can J Microbiol 41:303–309.

20. Matsusaki H, Manji S, Taguchi K, Kato M, Fukui T, Doi Y. 1998. Cloning and Molecular Analysis of the Poly(3-hydroxybutyrate) and Poly(3-hydroxybutyrate-co-3-hydroxyalkanoate) Biosynthesis Genes in Pseudomonas sp. Strain 61-3. J Bacteriol 180:6459–6467.

21. Phithakrotchanakoon C, Champreda V, Aiba S, Pootanakit K, Tanapongpipat S. 2013. Engineered *Escherichia coli* for Short-Chain-Length Medium-Chain-Length Polyhydroxyalkanoate Copolymer Biosynthesis from Glycerol and Dodecanoate. Biosci Biotechnol Biochem 77:1262–1268.

22. Lama L, Nicolaus B, Calandrelli V, Manca MC, Romano I, Gambacorta A. 1996. Effect of growth conditions on endo- and exopolymer biosynthesis in Anabaena cylindrica 10 C. Phytochemistry 42:655–659.

23. Panda B, Sharma L, Singh AK, Mallick N. 2008. Thin layer chromatographic detection of poly-beta-hydroxybutyrate (PHB) and poly-beta-hydroxyvalerate (PHV) in cyanobacteria. Indian J Biotechnol 7:230–234.

24. Bhati R, Mallick N. 2015. Poly(3-hydroxybutyrate-co-3-hydroxyvalerate) copolymer production by the diazotrophic cyanobacterium Nostoc muscorum Agardh: Process optimization and polymer characterization. Algal Res-Biomass Biofuels Bioprod 7:78–85.

25. Bresan S, Sznajder A, Hauf W, Forchhammer K, Pfeiffer D, Jendrossek D. 2016. Polyhydroxyalkanoate (PHA) Granules Have no Phospholipids. Sci Rep 6.

26. Panda B, Sharma L, Mallick N. 2005. Poly-beta-hydroxybutyrate accumulation in Nostoc muscorum and Spirulina platensis under phosphate limitation. J Plant Physiol 162:1376–1379.

27. Ansari S, Fatma T. 2016. Cyanobacterial Polyhydroxybutyrate (PHB): Screening, Optimization and Characterization. PLOS ONE 11:e0158168.

28. Taroncher-Oldenburg G, Nishina K, Stephanopoulos G. 2000. Identification and Analysis of the Polyhydroxyalkanoate-Specific β-Ketothiolase and Acetoacetyl Coenzyme A Reductase Genes in the Cyanobacterium Synechocystis sp. Strain PCC6803. Appl Environ Microbiol 66:4440–4448.

29. Hein S, Tran H, Steinbüchel A. 1998. Synechocystis sp. PCC6803 possesses a two-component polyhydroxyalkanoic acid synthase similar to that of anoxygenic purple sulfur bacteria. Arch Microbiol 170:162–170.

30. Kalia VC, Lal S, Cheema S. 2007. Insight in to the phylogeny of polyhydroxyalkanoate biosynthesis: horizontal gene transfer. Gene 389:19–26.

31. Talsness CE, Andrade AJM, Kuriyama SN, Taylor JA, vom Saal FS. 2009. Components of plastic: experimental studies in animals and relevance for human health. Philos Trans R Soc B Biol Sci 364:2079–2096.

32. Brandl H, Püchner P. 1991. Biodegradation of plastic bottles made from "Biopol" in an aquatic ecosystem under in situ conditions. Biodegradation 2:237–243.

33. Jendrossek D, Handrick R. 2002. Microbial Degradation of Polyhydroxyalkanoates. Annu Rev Microbiol 56:403–432.

34. Gonda KE, Jendrossek D, Molitoris HP. 2000. Fungal degradation of the thermoplastic polymer poly-β-hydroxybutyric acid (PHB) under simulated deep sea pressure. Hydrobiologia 426:173–183.

35. Matavulj M, Molitoris HP. 1992. Fungal degradation of polyhydroxyalkanoates and a semiquantitative assay for screening their degradation by terrestrial fungi. FEMS Microbiol Lett 103:323–331.

36. Balaji S, Gopi K, Muthuvelan B. 2013. A review on production of poly β hydroxybutyrates from cyanobacteria for the production of bio plastics. Algal Res 2:278–285.

37. Keshavarz T, Roy I. 2010. Polyhydroxyalkanoates: bioplastics with a green agenda. Curr Opin Microbiol 13:321–326.

38. Sureshkumar M. 2004. Production of biodegradable plastics from activated sludge generated from a food processing industrial wastewater treatment plant. Bioresour Technol 95:327–330.

39. Witholt B, Kessler B. 1999. Perspectives of medium chain length poly(hydroxyalkanoates), a versatile set of bacterial bioplastics. Curr Opin Biotechnol 10:279–285.

40. Chen G-Q. 2009. A microbial polyhydroxyalkanoates (PHA) based bio- and materials industry. Chem Soc Rev 38:2434–2446.

41. Kashiwaya Y, Takeshima T, Mori N, Nakashima K, Clarke K, Veech RL. 2000. d-β-Hydroxybutyrate protects neurons in models of Alzheimer's and Parkinson's disease. Proc Natl Acad Sci 97:5440–5444.

42. Massieu L, Haces M., Montiel T, Hernández-Fonseca K. 2003. Acetoacetate protects hippocampal neurons against glutamate-mediated neuronal damage during glycolysis inhibition. Neuroscience 120:365–378.

43. Tieu K, Perier C, Caspersen C, Teismann P, Wu D-C, Yan S-D, Naini A, Vila M, Jackson-Lewis V, Ramasamy R, Przedborski S. 2003. D-β-Hydroxybutyrate rescues mitochondrial respiration and mitigates features of Parkinson disease.

44. Zou X-H, Li H-M, Wang S, Leski M, Yao Y-C, Yang X-D, Huang Q-J, Chen G-Q. 2009. The effect of 3-hydroxybutyrate methyl ester on learning and memory in mice. Biomaterials 30:1532–1541.

45. A. Peterson A, Vogel F, P. Lachance R, Fröling M, Michael J. Antal J, W. Tester J. 2008. Thermochemical biofuel production in hydrothermal media: A review of sub- and supercritical water technologies. Energy Environ Sci 1:32–65.

46. Jazrawi C, Biller P, Ross AB, Montoya A, Maschmeyer T, Haynes BS. 2013. Pilot plant testing of continuous hydrothermal liquefaction of microalgae. Algal Res 2:268–277.

47. Liu X, Saydah B, Eranki P, Colosi LM, Greg Mitchell B, Rhodes J, Clarens AF. 2013. Pilot-scale data provide enhanced estimates of the life cycle energy and emissions profile of algae biofuels produced via hydrothermal liquefaction. Bioresour Technol 148:163–171.

48. Tran NH, Bartlett JR, Kannangara GSK, Milev AS, Volk H, Wilson MA. 2010. Catalytic upgrading of biorefinery oil from micro-algae. Fuel 89:265–274.

49. Murphy DJ. 2012. The dynamic roles of intracellular lipid droplets: from archaea to mammals. Protoplasma 249:541–585.

50. Georgianna DR, Mayfield SP. 2012. Exploiting diversity and synthetic biology for the production of algal biofuels. Nature 488:329–335.

51. Griffiths MJ, Harrison STL. 2009. Lipid productivity as a key characteristic for choosing algal species for biodiesel production. J Appl Phycol 21:493–507.

52. Liu X, Sheng J, Iii RC. 2011. Fatty acid production in genetically modified cyanobacteria. Proc Natl Acad Sci 108:6899–6904.

53. Schirmer A, Rude MA, Li X, Popova E, Cardayre SB del. 2010. Microbial Biosynthesis of Alkanes. Science 329:559–562.

54. Peramuna A, Morton R, Summers M. 2015. Enhancing Alkane Production in Cyanobacterial Lipid Droplets: A Model Platform for Industrially Relevant Compound Production. Life 5:1111–1126.

55. Wang W, Liu X, Lu X. 2013. Engineering cyanobacteria to improve photosynthetic production of alka(e)nes. Biotechnol Biofuels 6:69.

56. Chang Z, Flatt P, Gerwick WH, Nguyen V-A, Willis CL, Sherman DH. 2002. The barbamide biosynthetic gene cluster: a novel marine cyanobacterial system of mixed polyketide synthase (PKS)-non-ribosomal peptide synthetase (NRPS) origin involving an unusual trichloroleucyl starter unit. Gene 296:235–247.

57. Moffitt MC, Neilan BA. 2004. Characterization of the Nodularin Synthetase Gene Cluster and Proposed Theory of the Evolution of Cyanobacterial Hepatotoxins. Appl Environ Microbiol 70:6353–6362.

58. Orjala J, Gerwick WH. 1996. Barbamide, a Chlorinated Metabolite with Molluscicidal Activity from the Caribbean Cyanobacterium *Lyngbya majuscula*. J Nat Prod 59:427–430.

59. Tillett D, Dittmann E, Erhard M, von Döhren H, Börner T, Neilan BA. 2000. Structural organization of microcystin biosynthesis in Microcystis aeruginosa PCC7806: an integrated peptide–polyketide synthetase system. Chem Biol 7:753–764.

60. Li H, Sherman D, Bao S, Sherman L. 2001. Pattern of cyanophycin accumulation in nitrogen-fixing and non-nitrogen-fixing cyanobacteria. Arch Microbiol 176:9–18.

61. Liang B, Wu T-D, Sun H-J, Vali H, Guerquin-Kern J-L, Wang C-H, Bosak T. 2014. Cyanophycin Mediates the Accumulation and Storage of Fixed Carbon in Non-Heterocystous Filamentous Cyanobacteria from Coniform Mats. PLOS ONE 9:e88142.

62. Oppermann-Sanio FB, Steinbüchel A. 2002. Occurrence, functions and biosynthesis of polyamides in microorganisms and biotechnological production. Naturwissenschaften 89:11–22.

63. Singh RK, Tiwari SP, Rai AK, Mohapatra TM. 2011. Cyanobacteria: an emerging source for drug discovery. J Antibiot (Tokyo) 64:401–412.

64. Frommeyer M, Wiefel L, Steinbüchel A. 2016. Features of the biotechnologically relevant polyamide family "cyanophycins" and their biosynthesis in prokaryotes and eukaryotes. Crit Rev Biotechnol 36:153–164.

65. Füser G, Steinbüchel A. 2007. Analysis of Genome Sequences for Genes of Cyanophycin Metabolism: Identifying Putative Cyanophycin Metabolizing Prokaryotes. Macromol Biosci 7:278–296.

66. Simon RD. 1976. The biosynthesis of multi-l-arginyl-poly(l-aspartic acid) in the filamentous cyanobacterium Anabaena cylindrica. Biochim Biophys Acta BBA - Enzymol 422:407–418.

67. Ziegler K, Diener A, Herpin C, Richter R, Deutzmann R, Lockau W. 1998. Molecular characterization of cyanophycin synthetase, the enzyme catalyzing the biosynthesis of the cyanobacterial reserve material multi- L-arginyl-poly-L-aspartate (cyanophycin). Eur J Biochem 254:154–159.

68. Merritt MV, Sid SS, Mesh L, Allen MM. 1994. Variations in the amino acid composition of cyanophycin in the cyanobacterium Synechocystis sp. PCC 6308 as a function of growth conditions. Arch Microbiol 162:158–166.

69. Wingard LL, Miller SR, Sellker JML, Stenn E, Allen MM, Wood AM. 2002. Cyanophycin Production in a Phycoerythrin-Containing Marine Synechococcus Strain of Unusual Phylogenetic Affinity. Appl Environ Microbiol 68:1772–1777.

70. Picossi S, Valladares A, Flores E, Herrero A. 2004. Nitrogen-regulated Genes for the Metabolism of Cyanophycin, a Bacterial Nitrogen Reserve Polymer Expression and Mutational Analysis of Two Cyanophycin Synthetase and Cyanophycinase Gene Clusters in the Heterocyst-Forming Cyanobacterium Anabaena SP. PCC 7120. J Biol Chem 279:11582–11592.

71. Richter R, Hejazi M, Kraft R, Ziegler K, Lockau W. 1999. Cyanophycinase, a peptidase degrading the cyanobacterial reserve material multi-L-arginyl-poly-L-aspartic acid (cyanophycin). Eur J Biochem 263:163–169.

72. Obst M, Oppermann-Sanio FB, Luftmann H, Steinbüchel A. 2002. Isolation of Cyanophycin-degrading Bacteria, Cloning and Characterization of an Extracellular Cyanophycinase Gene (cphE) from Pseudomonas Anguilliseptica Strain BI the cphE Gene from P. Anguilliseptica BI encodes a Cyanophycin-Hydrolyzing Enzyme. J Biol Chem 277:25096–25105.

73. Joentgen W, Groth T, (u)}chel AS over, Hai T, Oppermann FB, Ag B. 1998. Polyasparaginic acid homopolymers an copolymers, biotechnical production and use thereof.

74. Ross RJ, Low K, Shannon JE. 1996. Polyaspartate Scale Inhibitors-Biodegradable Alternatives to Polyacrylates. NACE International.

75. Liu Z, Sun Y, Zhou X, Wu T, Tian Y, Wang Y. 2011. Synthesis and scale inhibitor performance of polyaspartic acid. J Environ Sci 23:S153–S155.

76. Gyarmati B, Mészár EZ, Kiss L, Deli MA, László K, Szilágyi A. 2015. Supermacroporous chemically cross-linked poly(aspartic acid) hydrogels. Acta Biomater 22:32–38.

77. Vega-Chacón J, Arbeláez MIA, Jorge JH, Marques RFC, Jafelicci M. 2017. pH-responsive poly(aspartic acid) hydrogel-coated magnetite nanoparticles for biomedical applications. Mater Sci Eng C 77:366–373.

78. Hai T, Hein S, Steinbüchel A. 2001. Multiple evidence for widespread and general occurrence of type-III PHA synthases in cyanobacteria and molecular characterization of the PHA synthases from two thermophilic cyanobacteria: Chlorogloeopsis fritschii PCC 6912 and Synechococcus sp. strain MA19. Microbiol Read Engl 147:3047–3060.

79. Charleston MA, Robertson DL. 2002. Preferential host switching by primate lentiviruses can account for phylogenetic similarity with the primate phylogeny. Syst Biol 51:528–535.

80. Conow C, Fielder D, Ovadia Y, Libeskind-Hadas R. 2010. Jane: a new tool for the cophylogeny reconstruction problem. Algorithms Mol Biol AMB 5:16.

81. Linton E, Rahman A, Viamajala S, Sims RC, Miller CD. 2012. Polyhydroxyalkanoate quantification in organic wastes and pure cultures using a single-step extraction and 1H NMR analysis. Water Sci Technol J Int Assoc Water Pollut Res 66:1000–1006.

82. Levering J, Broddrick J, Dupont CL, Peers G, Beeri K, Mayers J, Gallina AA, Allen AE, Palsson BO, Zengler K. 2016. Genome-Scale Model Reveals Metabolic Basis of Biomass Partitioning in a Model Diatom. PLOS ONE 11:e0155038.

83. Schoepp NG, Wong W, Mayfield SP, Burkart MD. 2015. Bulk solvent extraction of biomass slurries using a lipid trap. RSC Adv 5:57038–57044.

84. Simon RD. 1973. Measurement of the Cyanophycin Granule Polypeptide Contained in the Blue-Green Alga Anabaena cylindrica. J Bacteriol 114:1213–1216.

85. Broek TAB, McCarthy MD. 2014. A new approach to δ15N compound-specific amino acid trophic position measurements: preparative high pressure liquid chromatography technique for purifying underivatized amino acids for stable isotope analysis. Limnol Oceanogr Methods 12:840–852.

86. da Silva Malone CF, Rigonato J, Laughinghouse HD, Schmidt ÉC, Bouzon ZL, Wilmotte A, Fiore MF, Sant'Anna CL. 2015. Cephalothrix gen. nov. (Cyanobacteria): towards an intraspecific phylogenetic evaluation by multilocus analyses. Int J Syst Evol Microbiol 65:2993–3007.

87. Lehtimäki J, Lyra C, Suomalainen S, Sundman P, Rouhiainen L, Paulin L, Salkinoja-Salonen M, Sivonen K. 2000. Characterization of Nodularia strains, cyanobacteria from brackish waters, by genotypic and phenotypic methods. Int J Syst Evol Microbiol 50:1043–1053.

88. Voß B, Bolhuis H, Fewer DP, Kopf M, Möke F, Haas F, El-Shehawy R, Hayes P, Bergman B, Sivonen K, Dittmann E, Scanlan DJ, Hagemann M, Stal LJ, Hess WR. 2013. Insights into the Physiology and Ecology of the Brackish-Water-Adapted Cyanobacterium Nodularia spumigena CCY9414 Based on a Genome-Transcriptome Analysis. PLOS ONE 8:e60224.